Dynamical system theory and bifurcation analysis for microscopic traffic models

Bodo Werner
University of Hamburg
L'Aquila April 2010
2010 MathMods IP
mailto:werner@math.uni-hamburg.de

April 30, 2010

Abstract

Microscopic traffic follow-the-leader models are described by $2N$-dimensional nonlinear ODEs, where N is the number of cars. A prototype is given by [BHN+95].
In this lecture we present some background of dynamical system and bifurcation theory (see [Kuz98]) (Ch. 1-5) and of numerical bifurcation analysis (see [Gov00]) (Ch. 6) which is useful for a theoretical and numerical analysis of the traffic models in [GSW04, GW10, SGW09].
This will be applied to the traffic models which show a rich bifurcation scenario — Hopf bifurcations, folds and Neimark-Sacker bifurcation, especially when a circular road (periodic boundary conditions) with bottlenecks is considered (Ch. 7).

Contents

Chapter 1

ODEs

Let $f : D \to \mathbb{R}^n$ be smooth, $D \subset \mathbb{R}^n$ open. Initial value problem for an autonomous ODE:

$$\dot{x} = f(x), \quad x(0) = x_0 \in D.$$

Existence-uniqueness Theorem: There exists a unique (maximal) C^1-solution $u : J_u \to D$ on a maximal open interval J_u with $0 \in J_u$:

$$\dot{u}(t) = f(u(t)) \text{ for all } t \in J_u, \quad u(0) = x_0.$$

Phase curve / orbit:

$$\gamma := \{u(t) : t \in J_u\} \subset D$$

Integral curve:

$$\Gamma := \{(t, u(t)) : t \in J_u\} \subset J_u \times D$$

Geometry: $f(u(t))$ is tangential to the curve γ at $u(t)$.

1.1 Examples

1.1.1 Armament race

$$\dot{x} = -ax + by + r, \quad \dot{y} = cx - dy + s.$$

$b, c > 0$: fear parameters
$a, d > 0$: economical parameters
r, s: tendency parameters (pacifistic: < 0, militaristic: > 0)

ODE: $\dot{\mathbf{x}} = A\mathbf{x} + \beta$ with $\mathbf{x} = (x, y)$ and

$$A = \begin{pmatrix} -a & b \\ c & -d \end{pmatrix}, \quad \beta = (r, s)^t.$$

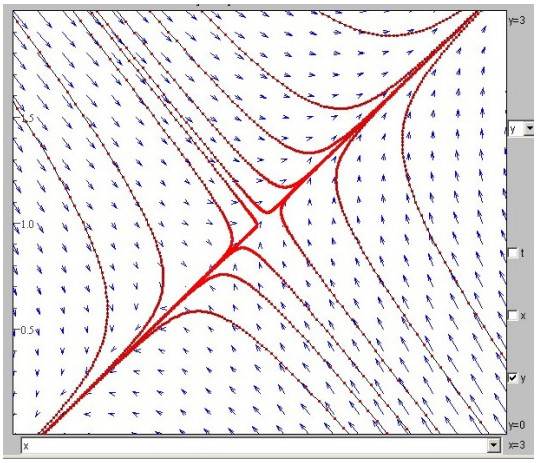

Figure 1.1: Phase portrait for $a = 2, b = 3, c = 5, d = 3, s = -2, r = -1$ with an equilibrium point (saddle)

For $a = 3, b = 2, c = 1, d = 2, r = s = 1$ we have an asymptotically stable equilibrium point

Remark: For plane systems is

$$Tr(A) < 0, \quad Det(A) > 0$$

necessary and sufficient for asymptotical stability. See also Ch. 2.2.1.

1.1.2 Nonlinear oscillations

$$m\ddot{x} + d(x)\dot{x} + D(x) = f(t)$$

$x(t)$: deflection of a mass point,
m: mass,
$d(x)$: (nonlinear) damping,
$D(x)$: restoring spring force,
$f(t)$: outer forcing

van der Pol oscillator:

$$\ddot{x} + \varepsilon(x^2 - 1)\dot{x} + x = 0, \varepsilon > 0$$

has a stable limit cycle

Duffing:

$$m\ddot{x} + d\dot{x} + c_1 c + c_3 x^3 = a\cos(\omega t)$$

(There are $2k\pi/\omega$–periodic ($k \in \mathbb{N}$) and irregular (chaotic) solutions).

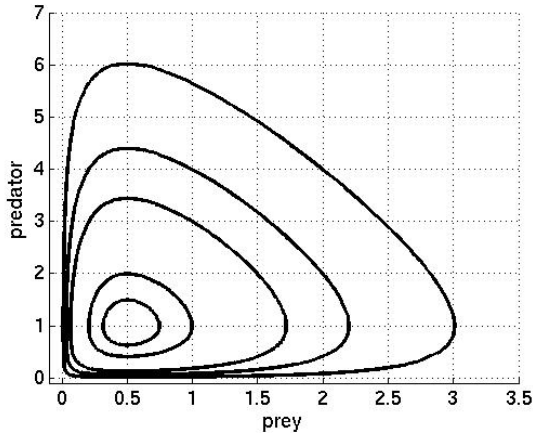

Figure 1.2: Phase portrait Lotka-Volterra ($a = 1, b = 1, c = 2, d = 1$)

1.1.3 Lotka–Volterra–System

Lotka (1925, 1880-1949) – Volterra (1931, 1860-1940)

$$\dot{x} = ax - bxy, \quad \dot{y} = cxy - dy.$$

(Parameters $a, b, c, d > 0$, $x(t)$= prey-, $y(t)$=predator density).
Two equilibria: $(0, 0)$ and $(d/c, a/b)$. See the phase portrait in figure 1.2.
There is an interesting historical background (fishing during the first world war in the Mediterranean)

1.1.4 Other predator prey systems

More realistic model (inner specific competition) :
Replacement of x by $\frac{ax}{b+x}$ (Michaelis–Menten, Holling):

$$\dot{x} = x\left[r\left(1 - \frac{x}{K}\right) - \frac{ay}{b+x}\right],$$
$$\dot{y} = y\left[e\frac{ax}{b+x} - d\right].$$

1.1.5 Chemical reactions

Noble prize winner (chemistry) 1977, Ilya Prigogine, 1917-2003, invented 1971 a very simple (theoretical) model which shows self-sustained periodic behaviour, called **Brusselator**:

$$A \to X, \quad 2X + Y \to 3X, \quad B + X \to Y + D, \quad X \to E$$

leads to

$$\dot{x} = A - (B+1)x + x^2 y, \quad \dot{y} = Bx - x^2 y$$

Equilibrium point $x_0 = A, y_0 = \frac{B}{A}$. There are periodic solutions due to Hopf bifurcation, see Ch. 6.4.1.

1.2 Microscopic Traffic Model - Basic Model

We will consider a microscopic car-following model, where N cars are moving along a straight road. Let $x_j(t) \in \mathbb{R}$ be the length car No. j has covered at time t. Assume that $x_1(t) < x_2(t) < \cdots < x_N(t)$ (no overtaking). Later (see Ch. 8) we will assume a circular road of length L and that $x_N(t) - x_1(t) < L$.
We assume that the driver of car No. j aims for some optimal velocity depending on its headway $y_j := x_{j+1} - x_j$ according to

$$\ddot{x}_j = \frac{1}{\tau_j}(V_j(x_{j+1} - x_j) - \dot{x}_j), \quad j = 1, \ldots, N-1. \tag{1.1}$$

Here V_j is an **optimal velocity function** for car No. j, see Ch. 8.1.1, and $\tau_j > 0$ are certain relaxation parameters which model the reaction time. For this model (1.1), the leading car (No. N) dynamics must be prescribed.
Let be $N = 2$ and let the leading car run with $x_2(t) = h(t)$, for instance $h(t) = t + 1$ (constant velocity):

$$\ddot{x} = V(h(t) - x) - \dot{x},\ x(0) = 0,\ \dot{x}(0) = v_0 > 0.$$

$x(t) = x_1(t)$ is the distance the second car has covered until time t. The dynamics is rather simple, see figure 1.3 for the first study of the influence of the parameters a and τ.
The dynamics is much richer if we assume periodic boundary conditions, i.e. we have a circular road (as in our papers [GSW04], [SGW09], [GW10]), see Ch. 8.

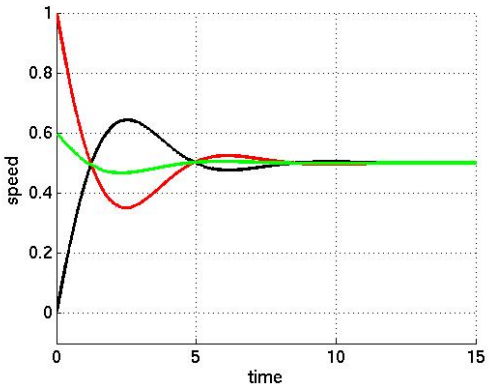

(a) $a = 2, \tau = 1$: speed

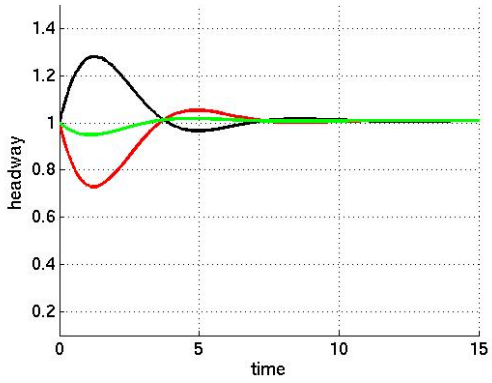

(b) $a = 2, \tau = 1$: headway

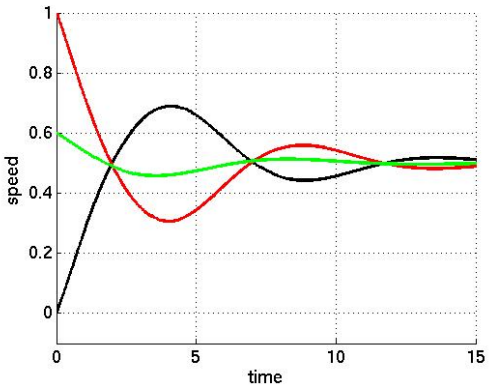

(c) $a = 2, \tau = 2$: speed

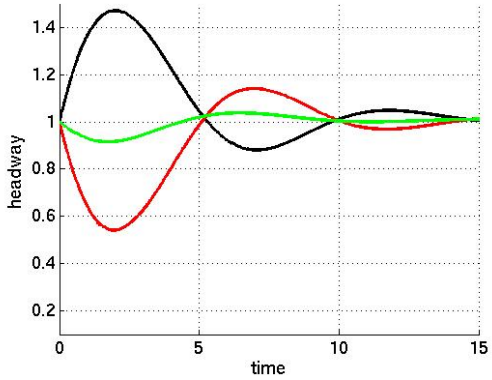

(d) $a = 2, \tau = 2$: headway

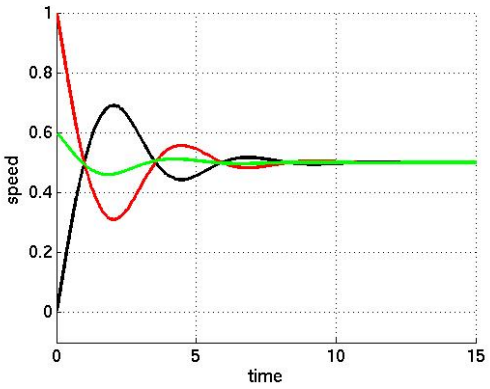

(e) $a = 4, \tau = 1$: speed

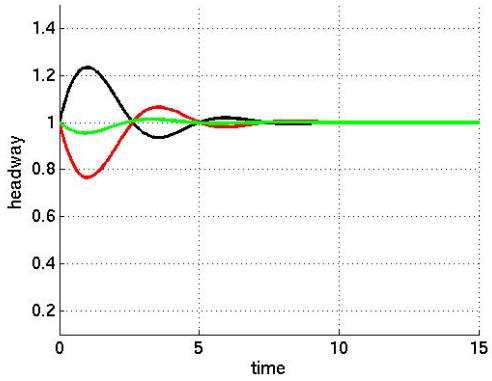

(f) $a = 4, \tau = 1$: headway

Figure 1.3: Leading car: $h(t) = 0.5t + 1$. Three different initial speeds and $x = 0$

Chapter 2

Dynamical Systems

We consider the initial value problem for an autonomous ODE,

$$\dot{x} = f(x), \quad x(0) = x_0 \tag{2.1}$$

with $f \in C^1(D, \mathbb{R}^n)$, $D \subset \mathbb{R}^n$ open, $x_0 \in D$.
There exists a unique maximal solution $u : J(x_0) \to \mathbb{R}^n$.

Dependence on x_0? Notation:

$$u(t) =: \varphi(t, x_0) \text{ or } u(t) = \varphi^t(x_0), \quad t \in J(x_0) =: (t^-(x_0), t^+(x_0)).$$

2.1 Flow

Lemma 2.1. *If $u(t)$ solves $\dot{x} = f(x)$, so does also $v(t) := u(t - c)$ for any phase shift $c \in \mathbb{R}$.*

We call $\varphi : D_\varphi \to D$ the **flow** of $\dot{x} = f(x)$, where

$$D_\varphi := \{(t, x) : x \in D, t \in J(x)\}.$$

Note that

$$\varphi_t(t, x) \,(:= \frac{\partial \varphi}{\partial t}(t, x)) = f(\varphi(t, x)).$$

2.1.1 Properties of the flow

Theorem 2.2.

$$D_\varphi \subset \mathbb{R} \times \mathbb{R}^n \text{ is open,} \tag{2.2}$$

$$\varphi : D_\varphi \to D \text{ is continuously-differentiable} \tag{2.3}$$

$$\{0\} \times D \subset D_\varphi, \quad \varphi(0, x) = x \text{ for all } x \in D, \tag{2.4}$$

$$x \in D, t \in J(x), s \in J(\varphi(t, x)) \Longrightarrow s + t \in J(x), \quad \varphi(s + t, x) = \varphi(s, \varphi(t, x)). \tag{2.5}$$

Remark: If $J(x) = \mathbb{R}$ for all $x \in D$, then $\varphi^t := \varphi(t, \cdot)$ are diffeomorphisms of D. We have $\varphi^0 = Id$ and $\varphi^{s+t} = \varphi^t \circ \varphi^s$.
From now on we write $\varphi^t(x)$ instead of $\varphi(t, x)$.

2.1.2 Dynamical system

Let $D \subset \mathbb{R}^n$ be nonempty and open. For all $x \in D$ there may be an open interval $J(x)$ with $0 \in J(x)$. A map

$$\varphi : D_\varphi := \{(t, x) : x \in D,\, t \in J(x)\} \to D$$

with the properties of Theorem 2.2 is called a (continuous) **dynamical system** on D.

Remarks:
a) The flow of an autonomous ODE system with C^1-vector field $f(x)$ defines a dynamical system. Vice versa:
b) A dynamical system φ defines a vector field

$$f(x) := \varphi_t(0, x)$$

on D, satisfying

$$\frac{\partial}{\partial t}\varphi^t(x) = f(\varphi^(x)).$$

f is called *infinitesimal generator* of the flow. In this sense, $A \in \mathbb{R}^{n\times n}$ is infinitesimal generator of e^{tA}.

Remark: We will not distinguish between flows and dynamical systems.

The most important generalization is that to a **discrete dynamical system**, where time is only discrete ($\mathbb{Z}$ or $\mathbb{N}$ instead of $\mathbb{R}$) and the flow is given by a map $F : D \to \mathbb{R}^n$ like $F := \varphi^1(\cdot)$). See also Ch. 4.1.1.
Or: D is an open Riemannian manifold (instead of $D \subset \mathbb{R}^n$).

2.1.3 Flow for linear autonomous systems

A linear, homogeneous ODE-system with constant coefficients has the form $\dot{x} = Ax$ with $A \in \mathbb{R}^{n,n}$.
Here $D = \mathbb{R}^n$ and $J(x) = \mathbb{R}$ for all $x \in \mathbb{R}^n$. Moreover

$$\varphi^t(x) = e^{tA}x.$$

2.1.4 Orbits

The **state space** D contains **orbits (phase curves)**

$$\gamma(x_0) := \{\varphi^t(x_0) : t \in J(x_0)\}.$$

Theorem 2.3. *For each $x \in D$ there is a unique orbit $\gamma(x)$ containing x. $\gamma(x) \cap \gamma(y) \neq \emptyset$ implies that $\gamma(x) = \gamma(y)$.*

If $f(x) \neq 0$, then $f(x)$ is tangential to the curve $\gamma(x)$ at x.

Forward orbit

$$\gamma^+(x) := \{\varphi^t(x) : t \in [0, t^+(x))\}.$$

2.2 Equilibrium points

A zero of f is called **equilibrium point** (or only equilibrium or *critical point*) of $\dot{x} = f(x)$ respectively **fixed point** of the flow φ.

$f(x) = 0$ iff $J(x) = \mathbb{R}$ and $\varphi^t(x) = x$ for all $t \in \mathbb{R}$ iff $\gamma(x) = \{x\}$.

2.2.1 Stability, attractivity

An equilibrium point $x_0 \in D$ is called (locally) **attractive** iff there is $\varepsilon > 0$ such that for $x \in K(x_0, \varepsilon)$

$$t^+(x) = +\infty, \quad \varphi^t(x) \to x_0 \text{ for } t \to +\infty \tag{2.6}$$

holds. x_0 is called globally (on D) attractive, iff (2.6) holds for all $x \in D$.

x_0 is called **stable** iff for all $\varepsilon > 0$ there is $\delta > 0$, such that $t^+(x) = +\infty$ and

$$\|\varphi^t(x) - x_0\| \leq \varepsilon \text{ for all } t \geq 0$$

for all $x \in K(x_0, \delta)$.

An equilibrium point $x_0 \in D$ is called **unstable** if it is not stable.

An equilibrium point x_0 is called (locally, globally) **asymptotically stable** iff x_0 is stable and (locally, globally) attractive.

Simple example:

$$\dot{x} = a\Big(1 - \frac{x}{K}\Big)x, \qquad (a, K > 0)$$

$x_0 = K$ is asymptotically stable and $x_0 = 0$ is unstable.

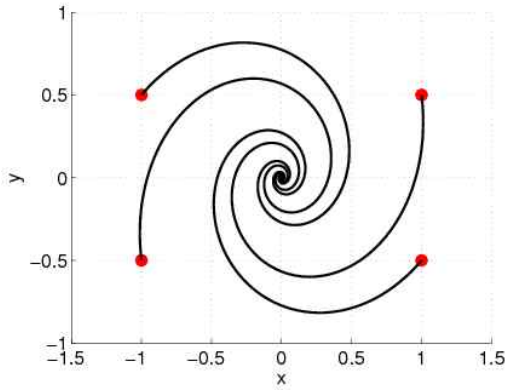

(a) Stable focus

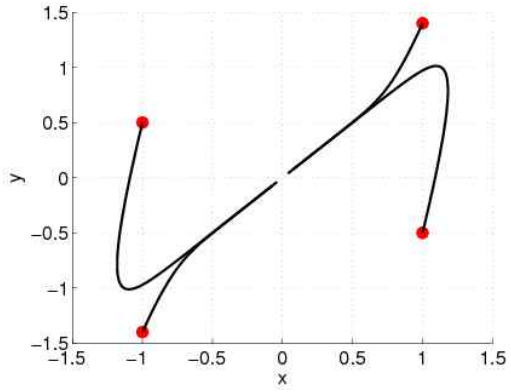

(b) Stable node

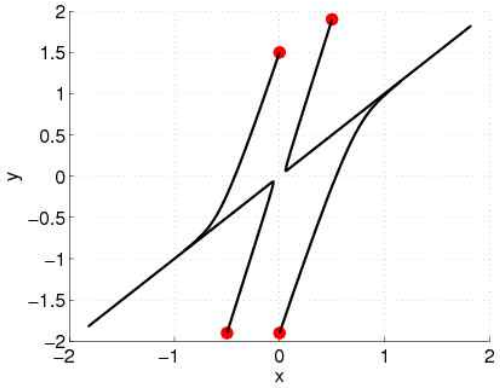

(c) Saddle

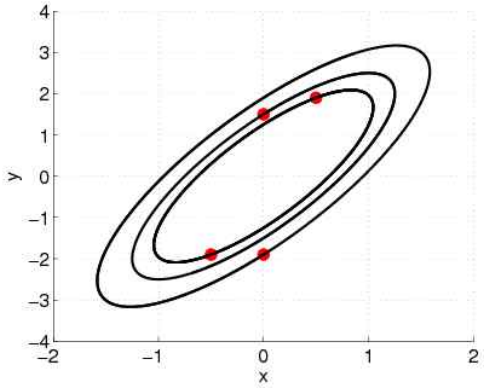

(d) Center

2.2.2 Autonomous linear systems

For $\dot{x} = Ax$ with $A \in \mathbb{R}^{n,n}$ there is the trivial equilibrium point $x_0 = 0$.

Theorem 2.4. *a) $x_0 = 0$ is (globally) asymptotically stable iff all eigenvalues of A have negative real part.*

b) If there is an eigenvalue of A with positive real part, then $x_0 = 0$ is unstable.

c) If all eigenvalues of A have non-positive real part, then $x_0 = 0$ is stable iff all eigenvalues with vanishing real part are semisimple.

2.2.3 Dependence on Initial Conditions and Parameters: Variational equations

Assume that $\dot{x} = f(x, \lambda)$ is given, where λ is a real parameter. f is assumed to depend smoothly on x and on λ. Let $u(t) := \varphi^t(x_0, \lambda_0)$ be the solution of an initial value problem

$\dot{x} = f(x, \lambda_0), x(0) = x_0$.

Theorem 2.5. *The derivatives*

$$Y(t) := \frac{\partial \varphi^t}{\partial x}(x, \lambda_0)\Big|_{x=x_0}, \quad z(t) := \frac{\partial \varphi^t}{\partial \lambda}(x_0, \lambda)\Big|_{\lambda=\lambda_0} \tag{2.7}$$

exist and solve so called (linear) variational equations

$$\dot{Y}(t) = A(t)Y(t), \quad Y(0) = E, \tag{2.8}$$

with

$$A(t) := \frac{\partial f}{\partial x}(x, \lambda_0)\Big|_{x=\varphi^t(x_0,\lambda_0)} \in I\!R^{n,n},$$

respectively

$$\dot{z}(t) = A(t)z(t) + g(t), \quad z(0) = 0, \tag{2.9}$$

with

$$g(t) := \frac{\partial f}{\partial \lambda}(\varphi^t(x_0, \lambda_0), \lambda)\Big|_{\lambda=\lambda_0}.$$

The special case that x_0 is an equilibrium point should be considered. Then $A(t)$ does not depend on t. If we forget λ, we have $A(t) = A = Df(x_0)$ – a matrix which is the core of the principle of linearized stability.

2.3 Periodic orbits

$x \in D$ is called a **periodic point** of the dynamical system[1] φ, respectively of $\dot{x} = f(x)$, iff x is not an equilibrium point and there is a (minimal) **period** $T > 0$ such that

$$\varphi(T, x) = x.$$

For periodic points x the orbit $\gamma(x)$ is a compact, closed curve. And vice versa. Each $y \in \gamma(x)$ is a T-periodic point. $\gamma(x)$ is called **periodic orbit** with period T.

The notions attractivity and (asymptotical) stability can be defined for periodic orbits in analogy to equilibrium points (*orbital* stability). The notion **limit cycle** is also used for asymptotically stable periodic orbits.

Classical example *van der Pol [1920]*:

$$\ddot{x} + \varepsilon(x^2 - 1)\dot{x} + x = 0, \quad \varepsilon > 0,$$

(s. figure 2.1).

[1] This makes also sense for discrete dynamical systems

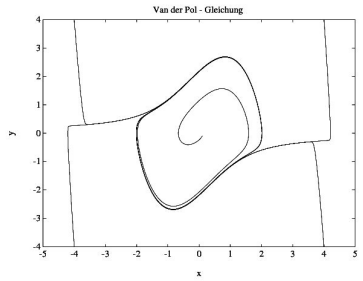

Figure 2.1: Phase curves for the van der Pol ODE with a limit cycle

2.4 Invariance, stability and attractivity of sets

2.4.1 Invariance

$M \subset D$ is (positive, forward) **invariant** iff

$$t^+(x) = +\infty,\ \varphi^t(x) \in M \ \text{ for all } x \in M, t \geq 0,$$

shortly iff

$$\varphi^t(M) \subset M \ \text{ for all } t \geq 0.$$

M is **strongly invariant** iff M is invariant and

$$\varphi^t(M) = M \ \text{ for all } t \geq 0.$$

2.4.2 Attractor

$x \in D$ is attracted by $M \subset D$, iff $t_+(x) = \infty$ and $\varphi^t(x) \to M$ for $t \to \infty$.
Inset(M): All points in D, which are attracted by M.
M is **attractive** or an **attractor**, iff inset(M) contains a neighborhood U of M.

Stability can be defined for invariant sets in analogy to equilibrium points.

2.5 Limit sets

ω-Limit set:

$$\mathcal{L}_\omega(x) := \{y \in \mathbb{R}^n : \exists (t_k) \to +\infty : \varphi^{t_k}(x) \to y\} \tag{2.10}$$

$$\mathcal{L}_\alpha(x) := \{y \in \mathbb{R}^n : \exists (t_k) \to -\infty : \varphi^{t_k}(x) \to y\} \tag{2.11}$$

Notation: $\omega(x)$ instead of $\mathcal{L}_\omega(x)$.
Remarks:

- $y \in \gamma(x)$ implies $\mathcal{L}_\omega(x) = \mathcal{L}_\omega(y)$.
- $\mathcal{L}_\omega(x) = \{x\}$ for an equilibrium point x.
- If x is an asymptotically stable equilibrium point, there is a neighborhood U of x with $\mathcal{L}_\omega(y) = \{x\}$ for all $y \in U$.
- $\mathcal{L}_\omega(x) = \gamma(x)$ for a periodic point x.

Theorem 2.6. *Let $\gamma^+(x)$ be contained in a compact $K \subset D$. Then $\mathcal{L}_\omega(x)$ is nonempty, compact, (positive und negative) invariant and connected.*
$M = \mathcal{L}_\omega(x)$ is the smallest compact set satisfying

$$\varphi^t(x) \to M \quad \text{for } t \to +\infty.$$

Corollary 2.7. *a) $\mathcal{L}_\omega(x) = \{y\}$ implies that $f(y) = 0$.*

b) If the periodic orbit $\gamma(x)$ is asymptotically stable, then there is a neighborhood U of $\gamma(x)$ with

$$\mathcal{L}_\omega(y) = \gamma(x) \text{ for all } y \in U.$$

Theorem 2.8 (Poincaré-Bendixson)**.** *Let $D = I\!R^2, x \in D$ and let the forward orbit $\gamma^+(x)$ be bounded. Let $\mathcal{L}_\omega(x)$ contain no equilibrium points. Then $\mathcal{L}_\omega(x)$ is a periodic orbit.*

2.6 Coordinate transformations, conjugacy

All reasonable definitions should be invariant under coordinate transformations.
Consider a C^∞-diffeomorphism $T : D_y \to D_x := D \subset \mathbb{R}^n$, shortly $x = T(y)$, respectively $y = S(x)$ with the inverse $S : D_x \to D_y$ of T. How is $\dot{x} = f(x)$ transformed into $\dot{y} = g(y)$?
From

$$\dot{x} = DT(y)\dot{y} = f(x) = f(T(y))$$

we obtain

$$\dot{y} = DT(y)^{-1} f(T(y)) =: g(y).$$

Now $DT(y)^{-1} = DS(T(y))$ and $g(y) = DS(T(y))f(T(y))$.
Of course, x_0 is an equilibrium point of $\dot{x} = f(x)$ iff $y_0 := S(x_0)$ is an equilibrium point of $\dot{y} = g(y)$.
An orbit $\gamma_x(x)$ of $\dot{x} = f(x)$ is transformed into an orbit $\gamma_y(Sx)$ of $\dot{y} = g(y)$. This follows from

$$\varphi_y(t, y) = S(\varphi_x(t, T(y))). \tag{2.12}$$

The two flows are diffeo-conjugate. The Jacobians $Df(x_0)$ and $Dg(y_0)$ with $x_0 = T(y_0)$ are similar for equilibrium points x_0 (and y_0).

The linear transformation $T(y) := Cy + b$ with a regular matrix C is an important special case. Then $S(x) = C^{-1}(x - b)$, and $\dot{y} = C^{-1} f(Cy + b)$, $\varphi_y^t(y) = C^{-1}((\varphi_x^t(Cy + b)) - b)$. This will be used in the proof of Theorem 3.1 (principle of the linearized stability.)

Chapter 3

Stability

3.1 Linearized stability

Let x_0 be an equilibrium point of $\dot{x} = f(x)$ and $A := Df(x_0)$ the Jacobian of f at x_0. There are two reasons to study

$$\dot{w} = Aw. \tag{3.1}$$

First, if $u(t)$ is a solution of $\dot{x} = f(x)$, then $w(t) := u(t) - x_0$ is a first-order solution of (3.1). Second, the solution of the linear matrix-ODE $\dot{Y} = AY, Y(0) = I$ equals $\frac{\partial \varphi}{\partial x}(t,x)\Big|_{x=x_0}$ for the flow for $\dot{x} = f(x)$. The linear system (3.1) is called *linearization* of $\dot{x} = f(x)$ at the equilibrium point x_0.

Does the (asymptotical) stability of $w_0 = 0$ for (3.1) imply the (asymptotical) stability of x_0 for $\dot{x} = f(x)$?

Theorem 3.1. *a) If all eigenvalues of A have negative real part, then x_0 is asymptotically stable.*
b) If there is an eigenvalue of A with positive real part, then x_0 is unstable.

Sketch of the proof of a):
Use $x = Cy + x_0$ with regular matrix C and study $\dot{y} = g(y)$ with $g(0) = 0$ and $A := Dg(0) = C^{-1}Df(x_0)C$.

Suitable choice of C: Assume $x_0 = 0$ and A is a special real ε-Jordan normal form — with $\varepsilon > 0$ instead of 1. Then $A = D + \varepsilon N$ with block-diagonal matrix D and nilpotent N. (D has 2×2-blocks for nonreal eigenvalues of A.) Our ODE can now be assumed to be $\dot{x} = f(x)$ with $f(x) = Ax + g(x)$ and $\|g(x)\| = o(\|x\|)$.
One can show that $V(x) := \frac{1}{2}(x^T x)$ is a strict Ljapunov function on a neighborhood of $x_0 = 0$ if $\varepsilon > 0$ is sufficiently small.

Remark: If all eigenvalues of A have non-positive real part, and there is at least one eigenvalue with vanishing real part, then x_0 might be stable or unstable.

3.1.1 Hyperbolic equilibrium points

An equilibrium point x_0 is called **hyperbolic**, iff all eigenvalues of $Df(x_0)$ have non vanishing real part.

Plane: saddle, node, sink, source

Locally flows of $\dot{x} = f(x)$ near x_0 and of $\dot{x} = Df(x_0)x$ near $w_0 = 0$ are topologically conjugate. The (un)stable manifold $M_s(x_0)$ ($M_u(x_0)$ of x_0 (for $\dot{x} = f(x)$) consists of all $x \in D$, for which $\varphi(t, x) \to x_0$ for $t \to +\infty$ ($t \to -\infty$).
The (un)stable manifold of $w_0 = 0$ (for $\dot{w} = Df(x_0)w$) is spanned by the generalized eigenspace E_s (E_u) with eigenvalues of negative (positive) real part. They are the tangent spaces of $M_s(x_0)$ ($M_u(x_0)$.

3.1.2 Linearized stability for fixed points

Let z_0 be fixed point of a C^1-map $F : D \to D$. Consider $M := DF(z_0)$ respectively the affine-linear map $G(x) := F(z_0) + DF(z_0)(x - z)$, the *linearisation* of f at z. The z is also fixed point of G. Or: $w = 0$ is fixed point of M. The stability of $w = 0$ is determined by the eigenvalues of M.

Theorem 3.2. *a) If all eigenvalues of M have modulus < 1, then z_0 is asymptotically stable.*

b) If there is an eigenvalue of M of modulus > 1, then z_0 is unstable.

z_0 is called hyperbolic fixed point, iff all eigenvalues of $DF(z)$ have modulus $\neq 1$.

Remark: An equilibrium point x_0 of $\dot{x} = f(x)$ is fixed point of the flow φ^t for all t. Observe that the eigenvalues of e^{tA} are obtained by $e^{t\lambda}$, where λ is eigenvalue of A and that $z \mapsto e^z$ maps the left complex plane into the interior of the complex unit circle.

Chapter 4

Periodic solutions of ODEs

In the sequel we write φ^t instead of $\varphi(t,.)$ and $F^t = F \circ F \circ \cdots \circ F$ for the t-multiple composition of a map F.

4.1 Introduction

4.1.1 Discrete dynamical systems

To analyze periodic solutions of ODEs it is very useful, even necessary, to understand discrete dynamical systems. They are defined by iteration of a **map** $F : A \subset \mathbb{R}^n \to \mathbb{R}^n$ with state space $\mathbb{R}^n$ (or manifolds), wehre the iteration index denotes a discrete time.

$$x^{k+1} = F(x^k), \quad k = 0, 1, 2, \ldots, \tag{4.1}$$

The starting vector x^0 plays an essential role. See Ch. 3.1.2, where we have discussed the stability of fixed points of F.
The *Flow* φ^t is given by $\varphi^t = F^t$ with $t \in \mathbb{N}_0$ or (if F is invertible) with $t \in \mathbb{Z}$.

z is called **p–periodic point** iff $F^p(z) = z$ and $p > 0$. The smallest integer $p > 0$ with this property is called (minimal–)**period**.
For $p = 1$ we have a **fixed point** of F ($F(z) = z$).

With z also $F^k(z), k \in \mathbb{N}_0$, is p–periodic. If p is the minimal-period, we get p different points for $k = 0, 1, ..., p-1$ which form the **p-periodic orbit**.

4.1.2 Periodic orbits of autonomous ODEs

For T–periodic solutions $u(t)$ of $\dot{x} = f(x)$ each point $z := u(t)$ satisfies $\varphi^T(z) = z$.
For $n = 1$ there cannot exist periodic solutions, in the plane case ($n = 2$) there is the famous Theorem 2.8 of Poincaré–Bendixson. Chaos and strange attractors are not possible.

4.1.3 Periodic solutions by periodic forcing

T–periodic (non-autonomous!) ODEs $\dot{x} = f(t, x)$ (defined by $f(t + T, x) = f(t, x)$ for all t and x) may have T-periodic (or $m \cdot T$-periodic) solutions. It is not surprising that a periodic forcing may produce a periodic answer.

4.1.4 Limit cycles

Often autonomous ODE-systems have solutions which converge against periodic solutions with an unknown period. We have seen such a behavior when we studied prey-predator-systems or the van-der-Pol oscillator (s. figure 2.1).

4.1.5 Stability

We will introduce so called *Floquet multipliers* of periodic solutions which determine the linearized stability in a similar way as the eigenvalues of the Jacobians $Df(x_0)$ for equilibria x_0.

4.1.6 Bifurcation

Dynamical systems often have *parameters* λ which influence the dynamics. Assume that a periodic solution looses its stability by variation of λ. What kind of solution will be observed instead of the (unstable) periodic one?

4.1.7 Classical books about Dynamical systems and bifurcation

R. Abraham, C. Shaw: Dynamics, the Geometry of Behavior I–IV, Aerial Press, 1982.
D.K. Arrowsmith, C.M. Place: An Introduction to Dynamical Systems, Cambridge University Press, 1990.
S.N. Chow, J. Hale: Methods of Bifurcation Theory, Springer, 1982.
R.L. Devaney: A first course in chaotic dynamical systems, Addison–Wesley, 1992.
M. Golubitsky, D.G. Schaeffer: Singularities and Groups in Bifurcation Theory (Volume 1). Springer, 1985.
M. Golubitsky, I.Stewart, D.G. Schaeffer: Singularities and Groups in Bifurcation Theory (Volume 2). Springer, 1988.
J. Guckenheimer, P. Holmes: Nonlinear Oscillations, Dynamical Systems and Bifurcation of Vector Fields, Springer, 1983.
J. Hale, H. Kocak: Dynamics and Bifurcation, Springer, 1991.
Y.A. Kuznetsov: Elements of Applied Bifuraction Theory, Springer, 1995.
J.P. La Salle: The Stability and Control of discrete Processes. Springer, 1986.
J.E. Marsden, M. Mc.Cracken: The Hopf bifurcation and its application, Springer, 1976.
H.E. Nusse, J.A. Yorke: Dynamics: Numerical explorations, Springer (1994).

4.2 Periodic orbits and solutions

4.2.1 Discrete systems

Each point z of a T-periodic orbit γ of $F : D \subset \mathbb{R}^n \to \mathbb{R}^n$ is fixed point of F^T (with integer T), the eigenvalues of $DF^T(z)$ enter. Though this matrix varies with z, all matrices $DF^T(z)$ turn out to be similar when z runs through γ. Hence the notion **eigenvalues of the periodic orbit** makes sense. Moreover, Theorem 3.2 is applicable. It not only determines the stability of the periodic points, but also that of the orbit as a set. This is the result of simple topological techniques:

Theorem 4.1. *Let z be a T-periodic point of F and γ the corresponding T-periodic orbit. Then γ is stable (asymptotically stable, unstable) iff z as fixed point of F^T is stable (asymptotically stable, unstable).*

4.2.2 Periodic solutions of periodic ODEs

Though we are mainly interested in periodic solutions of autonomous ODEs we have to study also non-autonomous (periodic) ODEs, since the linearisation of an autonomous ODE at a periodic solutions lead to time-periodic, linear ODEs.
Consider

$$\dot{x} = f(t, x), \quad f : \mathbb{R} \times D \to \mathbb{R}^n, \quad D \subset \mathbb{R}^n \text{ open} \tag{4.2}$$

with

$$f(t + T, x) = f(t, x) \quad \text{for all } (t, x) \in \mathbb{R} \times D$$

and a "period" $T > 0$.

Examples:

$$\dot{x} = A(t)x \tag{4.3}$$

with continuous $A : \mathbb{R} \to \mathbb{R}^{n,n}$ and periodicity $A(t + T) = A(t)$ for all $t \in \mathbb{R}$,

$$\dot{x} = A(t)x + b(t), \tag{4.4}$$

where $b(t + T) = b(t)$ for all t.

We have to take also the initial time t_0 in our focus.
Notation: $u(t) = \varphi(t, t_0, \xi)$ is the solution of (4.2) with initial condition $u(t_0) = \xi$. We have

$$\varphi(t, t_0, \xi) = \varphi(t + T, t_0 + T, \xi), \tag{4.5}$$

(If $u(t)$ solves (4.3), so does $v(t) := u(t + T)$).

The **time-T-map** $F(t_0; .)$ at t_0 is defined by

$$F(t_0; \xi) := \varphi(t_0 + T, t_0, \xi)$$

F defines a discrete dynamical system, which characterizes the behavior of (4.3).

Theorem 4.2. *A T-periodic ODE (4.2) has a T-periodic solution $u(t)$, iff $\xi_0 := u(t_0)$ is fixed point of the time-T-map $F(t_0; .)$:*

$$F(t_0; \xi_0) = \xi_0.$$

Set $t_0 = 0$ and $F := F(0; \cdot)$.

Let $F(\xi_0) = \xi_0$ and $u(t)$ the corresponding periodic solution. What about (the eigenvalues of) $DF(\xi_0)$? Variational equations for ODEs (Theorem 2.5) express the dependence of solutions of initial value problems on the initial values and on parameters by

$$DF(\xi_0) = \frac{\partial \varphi}{\partial x}(T, 0, x)\Big|_{x=\xi_0}.$$

With the *periodic* matrix

$$A(t) := \frac{\partial f}{\partial x}(t, x)\Big|_{x=u(t)} \in \mathbb{R}^{n,n}$$

and the periodic matrix-ODE

$$\dot{Y}(t) = A(t)Y(t), \quad Y(0) = I \tag{4.6}$$

we note that $DF(\xi_0) = Y(T)$. With other words: $DF(\xi_0)$ is the (linear!) time-T-map of the linear T-periodic system $\dot{y} = A(t)y$ for $t_0 = 0$. (Linearisation and time-T-map commute.) This is also important for the autonomous case $\dot{x} = f(x)$ where

$$DF(\xi_0) = \frac{\partial \varphi}{\partial x}(T, x)\Big|_{x=\xi_0}, \; A(t) := Df(x)|_{x=u(t)}.$$

Observe that $A(t)$ is time-variant for a periodic solution of an autonomous (time-invariant) ODE.

Definition 4.3. *The eigenvalues of the fixed point ξ_0 of the time-T-map F, i.e. the eigenvalues of $DF(\xi_0)$, are called* **Floquet multipliers**[1] *of the T-periodic solution $u(t)$.*

Remark 4.4. *Choosing an initial time $t_0 \neq 0$ we obtain similar matrices and hence the same eigenvalues.*

The solution $M := Y(T)$ of (4.6) is called **monodromy matrix** *or principal fundamental matrix of the T-periodic, linear, homogeneous system $\dot{y} = A(t)y$. The eigenvalues of M are*

[1] Gaston Floquet, 1847-1920.

called the Floquet multipliers of $\dot{y} = A(t)y$. In the sense above they are the Floquet multipliers of its trivial (T-periodic) solution $y(t) \equiv 0$.

The Lyapunov-Stability of periodic solutions makes sense for time-variant systems, not for autonomous systems. It is equivalent with the stability of the corresponding fixed point of the time-T-map.
Periodic solutions of $\dot{x} = f(x)$ are never asymptotically Lyapunov stable and never Lyapunov-hyperbolic. Here only the orbital stability and the orbital hyperbolicity make sense.

4.2.3 Periodic orbits of autonomous systems

Let $u(t)$ be a T-periodic solution of $\dot{x} = f(x)$ and let γ be the corresponding periodic orbit.
By def. 4.3 **Floquet multipliers** of $u(t)$ are defined.
With $u(t)$, also $v(t) := u(t - c)$ is a T-periodic solution (with phase shift c). One can show that $u(t)$ as well $v(t)$ have the same Floquet multipliers, hence the **Floquet multipliers of a T-periodic orbit** are well defined.

Theorem 4.5. *Let γ be a T-periodic orbit of an autonomous system $\dot{x} = f(x)$.*

a) Each $z \in \gamma$ is fixed point of the time-T-map F.

b) For all $z \in \gamma$ we have $DF(z)f(z) = f(z)$.
At least one Floquet multiplier of γ equals 1.

Proof: From $F(u(t)) \equiv u(t)$ and

$$DF(u(t))\dot{u}(t) = \dot{u}(t),$$

for all t, obviously $\xi := \dot{u}(t)$ is an eigenvector of $DF(u(t))$ with eigenvalue $\mu = 1$. ∎

Hence the principle of linearized *Lyapunov-* stability does not apply. The right concept is that of the *orbital* stability as defined in Ch. 2.3 .

4.2.4 Poincaré-maps for autonomous systems

Instead of the time-T-map (where we do not know the period T) we use Poincaré-maps. Their fixed points will correspond with periodic orbits, as a byproduct we get the (unknown) period as a *return time* of the fixed point.

We will remove the annoying Floquet multiplier $\mu = 1$ by considering an $n - 1$-dimensional subspace H, complementary to the tangent vector $f(z)$ to γ at point $z \in \gamma$.

In the sequel we denote the scalar product in $\mathbb{R}^n$ by $< u, v >:= u^t v$.

A hyperplane $z + H$ is called **transversal** in $z \in \gamma$, iff

$$\mathbb{R}^n = \langle f(z) \rangle \oplus H,$$

where $\langle v \rangle$ is the 1-dimensional subspace spanned by v.

Figure 4.1: H. Poincaré(1854-1912)

Lemma 4.6. *Let be H the hyperplane*

$$H := \{x \in I\!R^n :< w, x >= 0\} \quad \textit{for some } w \neq 0.$$

Then $z + H$ is transversal in $z \in \gamma$ iff

$$< w, f(z) >\neq 0. \tag{4.7}$$

A H-neighborhood $U \subset z + H$ of z is called a **local transversal section** of the orbit γ in z, iff

$$< w, f(x) >\neq 0 \quad \text{for all } x \in U. \tag{4.8}$$

By continuity, for each transversal hyperplane for z there is always a local, transversal section.

Theorem 4.7. *Let γ be a T-periodic orbit of $\dot{x} = f(x)$ and let $z+H$ be a transversal hyperplane in $z \in \gamma$. Then the following holds.*

There is a local transversal section U of γ in z and a real function $\tau : U \to I\!R$ with the properties:

- $\tau(z) = T$
- $\varphi^{\tau(x)}(x) \in z + H$ *for all* $x \in U$.
- τ *is continuously differentiable.*

The **return time** $\tau(x)$ *is unique in the following sense: The neighborhood U can be chosen in such a way, that there is an $\varepsilon > 0$, such that*

$$x \in U, \quad \varphi^t(x) \in z + H, \quad |t - T| < \varepsilon$$

imply that $t = \tau(x)$.

The **Poincaré-map**

$$\Pi : U \to z + H, \quad x \mapsto \varphi^{\tau(x)}(x)$$

is continuously differentiable and has z as fixed point.

Proof: Apply IFT on $g(x,t) = 0$ with

$$g(x,t) :=< w, (\varphi^t(x) - z) >, \quad g : \mathbb{R}^n \times \mathbb{R} \to \mathbb{R}$$

using $g(T,z) = 0$. ∎

Theorem 4.8. *For each Poincaré-map, the $n-1$ eigenvalues of $D\Pi(z)$ together with $\mu = 1$ are the n Floquet multipliers of the periodic orbit.*

Proof: Different Poincaré-maps are C^1-conjugate. Choose a very special hyperplane, for which $D\Pi(z)$ is a diagonal block in $DF(z)$, where F is the time-T-map. ∎

Orbital Stability

Theorem 4.9. *Let γ be a periodic orbit and Π a Poincaré-map for $z \in \gamma$. Then γ is orbital (asymptotically, un-)stable, iff z is an (asymptotically, un-)stable fixed point of Π.*

Theorem 4.10. *Let $\mu = 1$ be an algebraically simple Floquet multiplier of a periodic orbit γ.*

a) If all other Floquet multipliers have modulus < 1, then γ asymptotically stable.

b) If there is a Floquet multiplier of modulus > 1, then γ is unstable.

We call a periodic orbit γ **hyperbolic**, iff all Floquet multipliers except $\mu = 1$ have modulus $\neq 1$ and $\mu = 1$ is algebraically simple. γ is hyperbolic iff any Poincaré-map has a hyperbolic fixed point.

Remark: A periodic orbit of the mathematical pendulum is not hyperbolic (because of the Hamilton structure). But the periodic orbits are stable.

Chapter 5

Circle maps

5.1 Definition of circle maps

$S^1 := \mathbb{R}/\mathbb{Z}$ is the notation for a circle, identified with $S^1 = [0, 1]$, where the endpoints of the interval are identified.
We will consider orientation preserving diffeomorphisms $f : S^1 \to S^1$. The simplest examples are rotations

$$R_\omega : S^1 \to S^1, \quad \varphi \mapsto \varphi + \omega \bmod 1.$$

The reason to consider such maps are the cycles in Ch. 6.5 invariant under a map $F : \mathbb{R}^n \to \mathbb{R}^n$. The restriction of F to an invariant curve γ may be described by a circle map.

The basic theory can be found in Arnol'd [Arn88], de Melo, van Strien [dMvS91], Guckenheimer-Holmes [GH83].

5.2 Lift

$F : \mathbb{R} \to \mathbb{R}$ is called **Lift** of f iff

$$f \circ P = P \circ F, \tag{5.1}$$

where $P : \mathbb{R} \to S^1, x \mapsto x \bmod 1$ is a projection which winds $\mathbb{R}$ around the circle.
A lift is unique up to a constant ($F(x) = G(x) + k$ for all $x \in \mathbb{R}$). f is an **orientation preserving diffeomorphism** iff there is a Lift F satisfying $F(x + 1) = F(x) + 1$ (winding number $= 1$) and $F'(x) > 0$ for all x. Then $x \mapsto F(x) - x$ is 1-periodic.
$F(x) - x$ can be interpreted as the angle, about which f rotates $\xi := x \bmod 1$.

f defines a discrete dynamical system on S^1, especially an orbit (ξ_k) with

$$\xi_{k+1} = f(\xi_k), k = 0, 1, 2, ...$$

makes sense, as well as an orbit under a lift F. ξ is a q-periodic point of f iff there is $p \in \mathbb{N}_0$ with $F^q(\xi) = \xi + p$. Interpretation: p is the number of S^1-rounds the orbit of f has covered.

If q is minimal, then p and q have to be prime. We will see that the rational number $\frac{p}{q}$ is the rotation number of f in this periodic case.

5.3 Rotation number

We have seen that $\varphi(x) := F(x) - x$ is a rotation angle. Furthermore,

$$\varphi_k(x) := F^k(x) - x, k = 1, 2, ...$$

is the sum of k rotation angles along the first k iterates of the orbit of f, and $\varphi_k(x)/k$ is the average of these k angles.

Theorem 5.1. *Let F be a lift of f. Then*

$$\varrho_0(F) := \lim_{k\to\infty} \varphi_k(x)/k \tag{5.2}$$

exists, is independent of x and is unique up to a constant integer. Moreover,

$$\varrho_0(F) = \lim_{k\to\infty} F^k(x)/k. \tag{5.3}$$

Definition 5.2.

$$\varrho(f) := \varrho_0(F) \quad mod 1$$

is the **rotation number** *of f.*

There is an alternative way to look at the rotation number. Consider for any $y \in S^1$ the S^1–interval $I := [y, f(y))$. Now count the number of hits of I by an orbit, starting at any $\xi \in S^1$. The relative frequency of the hits converges against the rotation number! Hence $\varrho(f)$ is the *visiting probability* of $I := [y, f(y))$ by any orbit.

5.3.1 Rational and irrational rotation numbers

In the sequel, for rational numbers $\frac{p}{q}$ we always assume that the integers p and q are prime. For rotations $f = r_\omega$, where

$$r_\omega(x) = x + \omega \mod 1, \quad \omega \in [0, 1),$$

a Lift is given by $F(x) = x + \omega$. Of course $\varrho(r_\omega) = \omega$ holds. If $\omega = p/q \in \mathbb{Q}$, then every point of S^1 is q–periodic under r_ω. But if ω irrational, then every orbit is dense in S^1 (Theorem of Jacobi, see Devaney [Dev92]).

What are the generalizations for any diffeos f?

Theorem 5.3. *$\varrho(f) = p/q \in \mathbb{Q}$ iff f has a q–periodic orbit, i.e. there is a lift F of f and $x \in [0,1)$ with*

$$F^q(x) = x + p.$$

The proof is based on the following Lemma

Lemma 5.4. *Let F be the lift of f, for which $\varrho(f) = \varrho_0(F)$. Then $\varrho(f) > p/q$ ($\varrho(f) < p/q$) iff*

$$F^q(x) > x + p \quad (\text{resp.} \quad F^q(x) < x + p) \text{ for all } x \in S^1. \tag{5.4}$$

Theorem 5.5. *$\varrho(f)$ depends continuously on f.*

5.4 Denjoy's Theorem

Problem: Are all orbits under f dense in S^1, if $\varrho(f)$ irrational?

Lemma 5.6. *Let f be C^2. If $\varrho := \varrho(f)$ irrational, then any orbit under f has the same ordering*[1] *as under the rotation r_ϱ. Both orbits are dense in S^1.*

Remark: Starting the orbits at $\xi \in S^1$, one should look at those discrete times q when the orbits pass ξ, say the number of rounds is p. The integers p and q must be the same for f and for the rotation r_ϱ. (Then $\varrho > \frac{p}{q}$.)

Theorem 5.7 (Denjoy 1937)**.** *If $f \in C^2$ and if $\varrho = \varrho(f)$ is irrational, then every orbit of f is dense in S^1.*
f is topologically conjugate to the rotation r_ϱ, i.e. there is an orientation preserving homeomorphism h of S^1, such that

$$h \circ f = r_\varrho \circ h.$$

Remark: If ϱ is "sufficiently irrational", i.e. it satisfies a certain Diophantine equation[2], then h is smooth.

This Theorem of Denjoy and the Birkhoff Ergodic Theorem (see 8.35in Ch. 8.4) will be used for the explanation of the macroscopic periodicity of quasi-POMs for our traffic model in Ch. 8.4.

[1] This means that whenever we stop the sequence at a discrete time n, the orbit point ϕ_j of f is the left (right) neighbor of ϕ_k iff $s_j := j \cdot \varrho \bmod 1$ is the left (right) neighbor of s_k.

[2] $\exists \varepsilon, c > 0 : \left|\varrho - \frac{p}{q}\right| \geq \frac{c}{q^{2+\varepsilon}} \forall p, q \in \mathbb{N}$.

Chapter 6

Bifurcations

6.1 Introduction

Consider parameter dependent continuous or discrete dynamical systems

$$\dot{x} = f(x, \lambda), \quad \text{resp.} \quad x^{(k+1)} = F(x^{(k)}, \lambda)$$

with C^1-functions f or F defined on $\mathbb{R}^n \times \mathbb{R}$, where λ is a real parameter. We are interested in the dependence of equilibria or fixed points and of their stability on the parameter λ.

Imprecise definition for *bifurcation* at $\lambda = \lambda_c \in \mathbb{R}$: In every neighborhood of λ_c there are two parameters λ_1 and λ_2 such that the dynamical systems (or flows) are *qualitatively different* for $\lambda = \lambda_1$ and for $\lambda = \lambda_2$.

Typical local bifurcation: The number of stable (unstable) equilibria or fixed points is different for $\lambda = \lambda_1$ and for $\lambda = \lambda_2$. This implies that there are non-hyperbolic equilibria or fixed points x_c for $\lambda = \lambda_c$ (there are purely imaginary eigenvalues of $f_x(x_c, \lambda_c)$ or eigenvalues of modulus one of $F_x(x_c, \lambda_c)$).

Codimension-1–bifurcations are those bifurcations which occur "generically" for one parameter λ and are structurally stable, i.e. they persist under small perturbations.
Examples: **Folds (limit points, turning points)**, defined by an eigenvalue $\mu = 0$ of an equilibrium point respectively by $\mu = 1$ of a fixed point (see Ch. 6.3), **Hopf points**, defined by a pair of purely imaginary eigenvalues (equilibrium points) (see Ch. 6.4), respectively (**Neimark-Sacker points**) by a pair of complex-conjugate eigenvalues (fixed points) of modulus 1 (see Ch. 6.5), and **period doubling** for fixed points, defined by an eigenvalue $\mu = -1$.

Remark:
The bridge between continuous dynamical systems given by ODEs and discrete dynamical systems is given by the flow φ^T for fixed period T or by so called Poincaré maps. Their fixed points correspond to periodic solutions of autonomous ODEs.

Higher codimension bifurcations occur for $k > 1$ parameters. We mention (for $k = 2$ parameters) *Hopf–steady state mode interaction*, *Takens–Bogdanov–bifurcation*, *Hopf–Hopf mode interaction*, *hysteresis point* (or *cubic fold*) and *degenerate Hopf points*.

6.2 Hyperbolic equilibria and fixed points

Why does local bifurcation only occur for non-hyperbolic equilibria (fixed points)?

Let x_0 be an equilibrium point of $\dot{x} = f(x, \lambda)$ for $\lambda = \lambda_0$ and let $A_0 := f_x(x_0, \lambda_0)$ be the Jacobian. Let A_0 be regular (we call x_0 **regular** or **non-degenerated** if $\mu = 0$ is no eigenvalue of A_0). Then, by the Implicit Function Theorem (IFT), there is a neighborhood U_0 of (x_0, λ_0) and a C^k-function[1] $x(\lambda)$, defined in a neighborhood of λ_0, such that $f(x, \lambda) = 0$ and $(x, \lambda) \in U$ imply that $x = x(\lambda)$. It follows the uniqueness of $x(\lambda)$ and $x(\lambda_0) = x_0$. There is a branch (path) $(\lambda, x(\lambda))$ of equilibria for $\lambda \in \Lambda := U_{\lambda_0}$ given by the graph of $x(\lambda)$.

Now set $A(\lambda) := f_x(x(\lambda), \lambda)$ for $\lambda \in \Lambda$. Then $A(\lambda)$ is a C^{k-1}-function from Λ to $\mathbb{R}^{n\times n}$. Observe that $A(\lambda)$ is a *continuous* family of $n \times n$-matrices $A(\lambda)$ with parameter λ. Hence, the eigenvalues of $A(\lambda)$ depend continuously on λ. If x_0 is *hyperbolic*, one can choose Λ so small, such that the number of stable and unstable eigenvalues of $A(\lambda)$ do not change for $\lambda \in \Lambda$ (and $x(\lambda)$ preserves to be hyperbolic). By a Theorem of Grobmann/Hartmann, the flows in a neighborhood of $x(\lambda)$ are topologically equivalent (*qualitatively* the same). For short: **There is no local bifurcation near hyperbolic equilibria**.

An analogue result holds for *regular fixed points*, defined by $1 \notin \sigma(A_0)$ (the *spectrum* of A_0) with $A_0 := F_x(x_0, \lambda_0)$. IFT can be applied to $F(x, \lambda) - x = 0$.

Remark: Consider the vector field as parameter in a Banach space. Apply a Banach space IFT. Then hyperbolic equilibrium points and fixed points are structurally stable, since a C^k-perturbation of the vector field leads to a C^k-perturbation of the equilibrium points (fixed points) and to a continuous perturbation of their eigenvalues (a C^k-perturbation of their algebraically simple eigenvalues).

6.3 Folds

We restrict our view to continuous dynamical systems. The simplest loss of hyperbolicity (or even of stability) occurs, if, for a specific parameter λ_0, an equilibrium point x_0 has a *singular* Jacobian $A_0 = f_x(x_0, \lambda_0)$. Then typically (generically) the following holds

- The rank deficiency is one, i.e. $\text{rank}(A_0)=n-1$ or – equivalently – $\dim \text{Ker}(A_0)=1$
- $f_\lambda(x_0, \lambda_0) \notin \mathcal{R}(A_0)$, where $\mathcal{R}(A_0)$ is the *Range* of A_0.

By these two *fold conditions*, a *fold* of $\dot{x} = f(x, \lambda)$ for $\lambda = \lambda_0$ is defined. Shortly: (x_0, λ_0) is a **fold** (or **limit point**). We are going to study the zeros of $f(x, \lambda) = 0$ in a neighborhood of a fold.
The two fold conditions imply $Rank(Df(x_0, \lambda_0)) = n$. Vice versa $Rank(Df(x_0, \lambda_0)) = n$ and the singularity of $f_x(x_0, \lambda_0)$ imply the two fold conditions.

[1] Assume $f \in C^k$.

What do we know about the global solution set $N_0 := \{(x,\lambda) : f(x,\lambda) = 0\}$ (or at least about the "local" solution set in the neighborhood of (x_0,λ_0))? Let be $f \in C^\infty(\mathbb{R}^{n+1},\mathbb{R}^n)$. Then by the so-called Sard-Theorem for almost all $y \in \mathbb{R}^n$ the solution set $N_z := \{z \in \mathbb{R}^{n+1} : f(z) = y\}$ is a one-dimensional C^∞-manifold. Hence we can generically expect that $y = 0$ is such generic choice and we have just a smooth curve N_0 in $\mathbb{R}^{n+1}$. How does the fold influence the shape of this curve?

Theorem 6.1. *Let x_0 be a fold for $\lambda = \lambda_0$. Then there is a neighborhood U of (x_0,λ_0) such that $f^{-1}(0) \cap U$ is a 1D-differentiable manifold (curve)*

$$\mathcal{C} = \{(x(s),\lambda(s)) : s \in J := (-\varepsilon,\varepsilon)\},\ \varepsilon > 0$$

with functions $x(s) \in C^1(J,\mathbb{R}^n)$, $\lambda(s) \in C^1(J,\mathbb{R})$, satisfying $x(0) = x_0$ and $\lambda(0) = \lambda_0, \lambda'(0) = 0$ (and $(x'(s),\lambda'(s)) \neq 0$ for all s).

Proof: Apply IFT in a suitable way.
Define

$$f_x^0 := f_x(x_0,\lambda_0), \quad f_\lambda^0 := f_\lambda(x_0,\lambda_0), \ldots$$

Differentiation of $f(x(s),\lambda(s)) \equiv 0$ by s at $s = 0$ yields

$$f_x^0 x'(0) + f_\lambda^0 \lambda'(0) = 0, \tag{6.1}$$

and the fold-conditions imply $\lambda'(0) = 0$, i.e., $s \mapsto \lambda(s)$ has an extremal point at $s = 0$. ∎

Definition 6.2. *Let x_0 be a fold for $\lambda = \lambda_0$. Assume additionally that $\lambda''(0) \neq 0$, i.e., $s \mapsto \lambda(s)$ has a strict minimum or maximum at $s = 0$. Then x_0 is called a* **quadratic fold** *for $\lambda = \lambda_0$.*

Talking about folds we always mean quadratic folds which have an obvious geometrical meaning, see figure 6.1.

Remark: At a fold, two equilibria are borne or die.

Theorem 6.3. *Let be $n = 1$. Then x_0 is a (quadratic) fold iff $f(x_0,\lambda_0) = 0$ and the three conditions*

$$f_x^0 = 0, \quad f_\lambda^0 \neq 0, \quad f_{xx}^0 \neq 0 \tag{6.2}$$

hold.

6.3.1 Stability

Theorem 6.4. *Let x_0 be a (quadratic) fold for $\lambda = \lambda_0$ and $\mathcal{C} = \{(x(s),\lambda(s)) : |s| < \varepsilon\}$ a branch of equilibria through (x_0,λ_0) (at $s = 0$). Set $d(s) := \det(f_x(x(s),\lambda(s)))$. Then $d(0) = 0$ and $d'(0) \neq 0$. Particularly $x(s)$ is hyperbolic for $s \neq 0$ if $|s|$ is sufficiently small and $\mu = 0$ is the only eigenvalue of f_x^0 on the imaginary axis.*

Stability change at a fold*: Let $x(s)$ be asymptotically stable for $s < 0$ (respectively for $s > 0$). Then $x(s)$ is unstable for $s > 0$ (resp. for $s > 0$).*

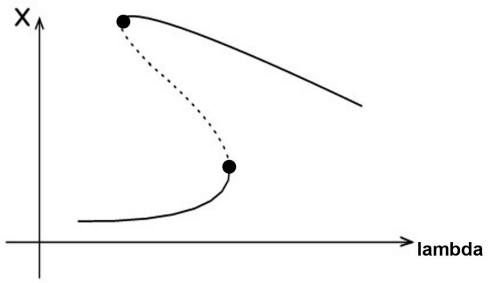

Figure 6.1: Two fold points

Typically (generically) $\mu = 0$ is an algebraically simple eigenvalue of f_x^0. A tricky application of IFT leads to

$$f_x(x(s), \lambda(s))u(s) = \mu(s)u(s)$$

with smooth eigenvalues $\mu(s)$ and eigenvectors $u(s) \neq 0$, satisfying $\mu(0) = 0$.
From $d'(0) \neq 0$ it follows that $\mu'(0) \neq 0$. Therefore, the fold-condition $\lambda''(0) \neq 0$ is a transversality condition for eigenvalues: An (real) eigenvalue curve $\mu(s)$ of $A(s) := f_x(x(s), \lambda(s))$ crosses the imaginary axis at $\mu = 0$ with non-zero speed.

Folds are also called **saddle-node bifurcation points**. Why? Assume that $\mu(s) < 0$ for $s < 0$ and that all other eigenvalues of $A(s)$ have negative real part. Then $x(s)$ is a stable node for $s < 0$, at least in the plane. For $s > 0$ we have $\mu(s) > 0$, the other eigenvalues may still remain in the left complex plane. Then for $n = 2$ the equilibrium must be a saddle. A node bifurcates to a saddle. Draw phase portraits for $s < 0$ and $s > 0$ (and $s = 0$). For $n = 1$ the situation is much simpler, see below.

6.3.2 Examples

Normal form:
Let $n = 1$ and $f(x, \lambda) = ax^2 - \lambda$, where a is a real parameter. We have a (quadratic) fold at $(x_0, \lambda_0) = (0, 0)$ iff $a \neq 0$. Draw the zero set in dependence of a and discuss the stability.

Prey-Predator system
Given

$$\begin{aligned} \dot{x} &= x(a - ex) - \tfrac{bxy}{1+rx} \\ \dot{y} &= \tfrac{cxy}{1+rx} - dy. \end{aligned} \tag{6.3}$$

with positive parameters. Note that $G(x) := \frac{x}{1+rx}$ tries to model the fact that the predator cannot "eat" arbitrary many preys.

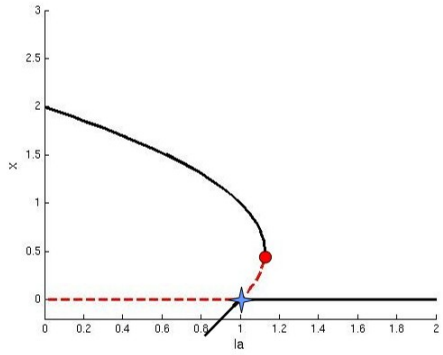

Figure 6.2: Solution diagram for (6.4): $a = 1, r = 1, e = 0.5, b = 1$

Consider the simple case that the predator is kept constant (the prey may be grass, the predator cattle which do not need the grass to survive). Then $\lambda := y$ is a further parameter, and one obtains the 1D-problem

$$\dot{x} = f(x, \lambda), \quad f(x, \lambda) := x(a - ex) - \frac{bx\lambda}{1 + rx}. \tag{6.4}$$

If $a \cdot r - e > 0$, then there is a quadratic fold at

$$\lambda = \lambda_0 := \frac{1}{b}\left(a + \frac{(ar - e)^2}{4er}\right),$$

characterizing a collapse for the grass for $\lambda > \lambda_0$ (too much cattle).
$x = 0$ is always an equilibrium point, which is asymptotically stable for large λ (no chance for the grass to survive). It is easy to see that at $\lambda_1 := \frac{a}{b}$ there is a stability change. For $\lambda < \lambda_1$ the no-grass-equilibrium $x = 0$ is unstable — the grass can survive, since there is not so much cattle. Using $a \cdot r - e > 0$, there exists a branch of positive equilibria with a quadratic fold at $\lambda = \lambda_0$ which bifurcates from λ_1. No positive equilibria exist for $\lambda > \lambda_0$, while for $\lambda < \lambda_0$ there are two equilibria, the larger one being stable, the other unstable. See figure 6.2.

Scalar logistic map

$$n = 1, \quad F(x) = a \cdot x(1 - x), \quad a > 0$$

defines a famous scalar discrete dynamical system with parameter $a > 0$.

The fixed point $x = 0$ looses its stability for $a = 1$ (*transcritical bifurcation* with eigenvalue 1), for $a > 1$ there bifurcates a branch of positive fixed points $x = 1 - \frac{1}{a}$ which looses its stability at $a = 3$ via period doubling, a stable 2–periodic orbit appears which undergoes another period doubling at $a = 3.4495$. Further period doubling bifurcations occur for $a = 3.5441$, $a = 3.5644$, $a = 3.5688$, etc. (Feigenbaum scenario).
Then, until $a = 4$, there are observed irregular dynamics ("Chaos") and "periodic windows", where stable periodic orbits live. The largest periodic window with period 3 starts at $a = 1 + 2\sqrt{2} = 3.82843$,

it follows a period doubling at $a = 3.84150$ with another Feigenbaum sequence. The next periodic window with period 5 starts at $a = 3.73817$. At $a = 3.74112$ there is the next period-doubling bifurcation. Most values have been obtained numerically.
The p-period windows seem to start at folds for fixed points of F^p, where p is the period: A couple of p-periodic orbits are borne, one stable, one unstable.

6.4 Hopf bifurcation

Let x_0 be a non-hyperbolic, but non-degenerate (regular) equilibrium point for $\lambda = \lambda_0$. Then $A_0 := f_x(x_0, \lambda_0)$ is regular and possesses a pair of imaginary eigenvalues.
Because of IFT there is a *branch* $\mathcal{C} = \{(x(\lambda), \lambda) : \lambda \in \Lambda\}$ of equilibria $x(\lambda)$, where $\Lambda = \{\lambda : |\lambda - \lambda_0| < \varepsilon\}$ is an open, λ_0 containing interval.
We assume that the two imaginary eigenvalues of A_0 are algebraically simple. Then Λ can be chosen such that there are algebraically simple eigenvalues

$$\mu(\lambda) := \alpha(\lambda) \pm i\beta(\lambda) \in \sigma(f_x(x(\lambda), \lambda)), \quad \lambda \in \Lambda,$$

with continuous-differentiable real functions $\alpha(\lambda)$ and $\beta(\lambda)$ satisfying

$$\alpha(\lambda_0) = 0, \quad \beta(\lambda_0) =: \omega_0 \neq 0.$$

Definition 6.5. *Let x_0 be a regular equilibrium point for $\lambda = \lambda_0$. x_0 is called* **Hopf–bifurcation point** *or shortly* **Hopf point** *for $\lambda = \lambda_0$, iff*

- **Eigenvalue condition:** *$f_x^0 := f_x(x_0, \lambda_0)$ has a pair of algebraically simple eigenvalues $\pm i\omega_0$ where $\omega_0 \neq 0$ and where $\mu = 0$ is no eigenvalue of f_x^0, i.e. x_0 is regular.*
- **Transversality condition (eigenvalue crossing condition)**

$$\alpha'(\lambda_0) \neq 0. \tag{6.5}$$

(The two eigenvalue curves $\alpha(\lambda) \pm i\beta(\lambda)$ cross the imaginary axis with non-zero speed).

Theorem 6.6. *(*E. Hopf *(1942),* Poincaré *(1892),* Andronov *(1926))*
Let x_0 be a Hopf–bifurcation point for $\lambda = \lambda_0$. Assume that $i\omega_0 \neq 0$ is an algebraically simple eigenvalue of f_x^0 with eigenvector $u_0 + iv_0$, $u_0, v_0 \in \mathbb{R}^n$.
Let $ik\omega_0, k = 0, 2, 3, 4, ...$, be no eigenvalues of f_x^0 (resonance condition).

Then there is a branch of $T(s)$-periodic solutions $u(t; s)$ (respectively $T(s)$-periodic orbits $\gamma(s)$) for parameter $\lambda = \lambda(s)$, parametrized by a parameter s which can be interpreted as an "amplitude" $(0 \leq s < \varepsilon)$ with the following properties.

- $T(s) = \frac{2\pi}{\omega_0} + O(s^2), \quad \lambda(s) = \lambda_0 + O(s^2),$

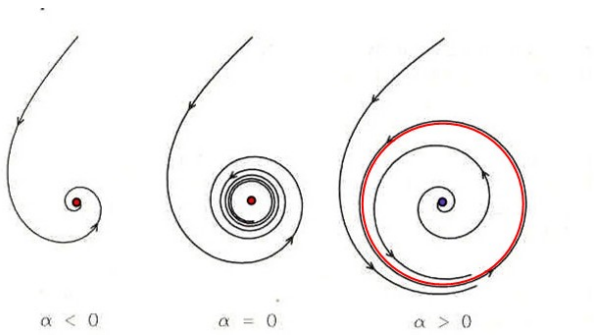

FIGURE 2.13. Hopf bifurcation

Figure 6.3: Supercritical (soft) Hopf bifurcation

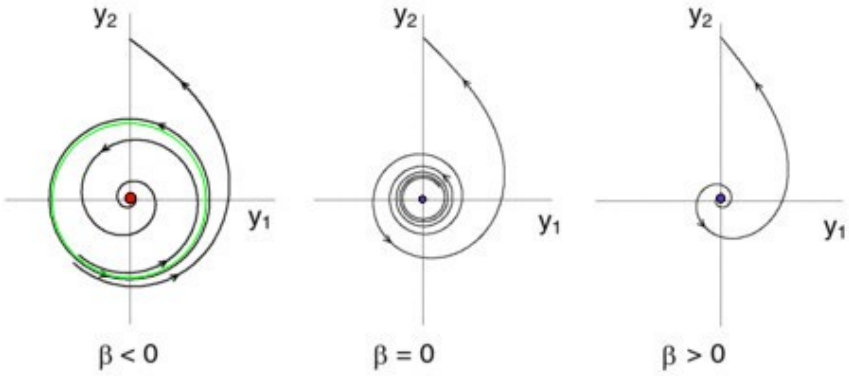

Figure 6.4: Subcritical (hard) Hopf bifurcation

- $u(t;s) = x_0 + s(\cos(\omega_0 t)u_0 - \sin(\omega_0 t)v_0) + O(s^2)$, *i.e. the periodic orbits are located in a neighborhood of* x_0, *and converge (shrink) for* $s \to 0$ *to the equilibrium point* x_0. *For small* s *the orbits are living with "first order accuracy" in the plane* $E := x_0 + H$, *where* H *is spanned by* u_0 *and* v_0 *(the so-called* **real eigenspace** *for the eigenvalues* $\pm i\omega_0$*).*
- $T(s)$, $\lambda(s)$ *and* $u(t;s)$ *depend continuously-differentiable on* s.
- *The periodic solutions are unique in the following sense:*

  There are neighborhoods U *of* x_0 *and* Λ *of* λ_0 *such that for* $\lambda \in \Lambda$ *and any periodic orbit* C *located in* U *there is a parameter* s *with* $C = \gamma(s)$ *and* $\lambda = \lambda(s)$.

One has to distinguish **supercritical** and **subcritical** Hopf–bifurcations, depending on the stability of the bifurcating periodic orbits (see figure 6.3-figure 6.4 as well as the examples). Conditions for super- or subcriticality are so called *nonlinearity conditions*. In figure 8.4 for our traffic model, both Hopf points seem to be subcritical. As a consequence, "large" stable periodic orbits coexist with stable equilibria, before they loose stability.

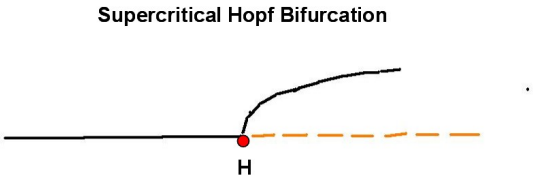

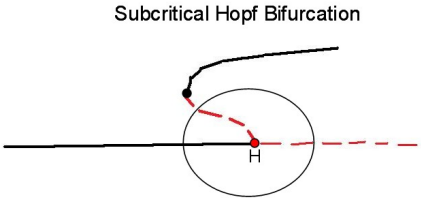

For a proof of the Hopf Theorem see MARSDEN–MCCRACKEN, where the plane situation ($n = 2$) is proved and where the general case is transformed into the plane case by center manifolds.

6.4.1 Examples

Normal form

This is a plane system which describes alls non-degenerate Hopf bifurcations (s. GUCKENHEIMER-HOLMES, S.152, WIGGINS, S.271).

$$\begin{pmatrix} \dot{x} \\ \dot{y} \end{pmatrix} = \begin{pmatrix} d\lambda + a(x^2+y^2) & -(\omega + c\lambda + b(x^2+y^2)) \\ \omega + c\lambda + b(x^2+y^2) & d\lambda + a(x^2+y^2) \end{pmatrix} \begin{pmatrix} x \\ y \end{pmatrix}. \tag{6.6}$$

There is a trivial branch $(x(\lambda), y(\lambda)) \equiv (0,0)$ of equilibria with Jacobians

$$J(\lambda) = \begin{pmatrix} d\lambda & -(\omega + c\lambda) \\ \omega + c\lambda & d\lambda \end{pmatrix}.$$

Let $d, \omega \neq 0$. Then $(x_H, y_H) = (0,0)$ and $\lambda_H = 0$ fulfill the eigenvalue condition for a Hopf bifurcation. ($d \neq 0$ is the transversality condition).
The bifurcation period solutions and their stability can easily been studied by using polar coordinates.

$$\dot{r} = (d\lambda + ar^2)r, \quad \dot{\vartheta} = \omega + c\lambda + br^2.$$

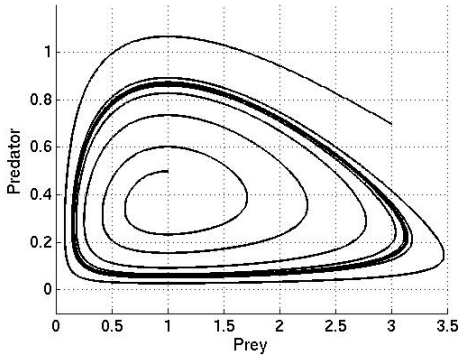

Figure 6.5: Limit cycle for the Bazykin model $r = 1$, $b = 1$, $d = 1$, $a = 4$, $e = 0.5, K = 4$

Periodic solutions correspond with non-trivial equilibria of the scalar ODE $\dot{r} = (d\lambda + ar^2)r$, their orbits are circles. They are (asymptotically) stable iff the equilibria are.
If $d > 0$, the trivial equilibria are stable for $\lambda < \lambda_H = 0$, unstable for $\lambda > \lambda_H$. If $a < 0$, there exist asymptotically stable periodic orbits for $\lambda > \lambda_H$ in form of circles with radii $\sqrt{-d\lambda/a}$. We have a so called *supercritical (soft)* Hopf bifurcation, s. figure 7.27 in HALE-KOCAK.
In contrast to this the case $d > 0, a > 0$ leads to a *subcritical (hard)* bifurcation (s. figure 3.7, 3.8 in KUZNETSOV), periodic orbits exist for $\lambda < \lambda_H$ and are unstable.
For $a = 0$ the bifurcation is "'vertical"', this is a degenerate Hopf bifurcation.

Observe that the branch of periodic solutions can be parametrized by the amplitude $s := r$.

Predator-Prey System

Bazykin model:

$$\dot{x} = x\left[r\left(1 - \frac{x}{K}\right) - \frac{ay}{b+x}\right],$$
$$\dot{y} = y\left[e\frac{ax}{b+x} - d\right]$$

for

$$r = 1, b = 1, d = 1, a = 4, e = 0.5.$$

For $K > 1$ there are unique positive equilibria $(1, \frac{1}{2} - \frac{1}{2K})$ being a stable equilibrium point for $1 < K < 3$, and an unstable focus for $K > 3$ — at $K = 3$ there is a Hopf bifurcation! Numerically we found stable periodic orbits for $K > 3$(s. figure 6.5 for $K = 9$), which is the result of a supercritical Hopf bifurcation.

Brusselator

Ch. 1.1.5:

$$\dot{x} = A - (B+1)x + x^2y, \quad \dot{y} = Bx - x^2y$$

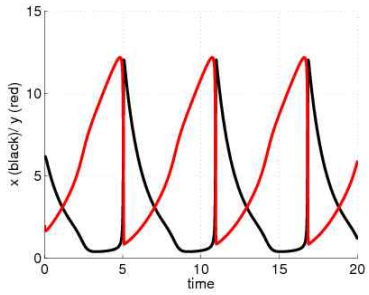

Figure 6.6: Periodic solutions of the Brusselator for $A = 2.90, B = 10$

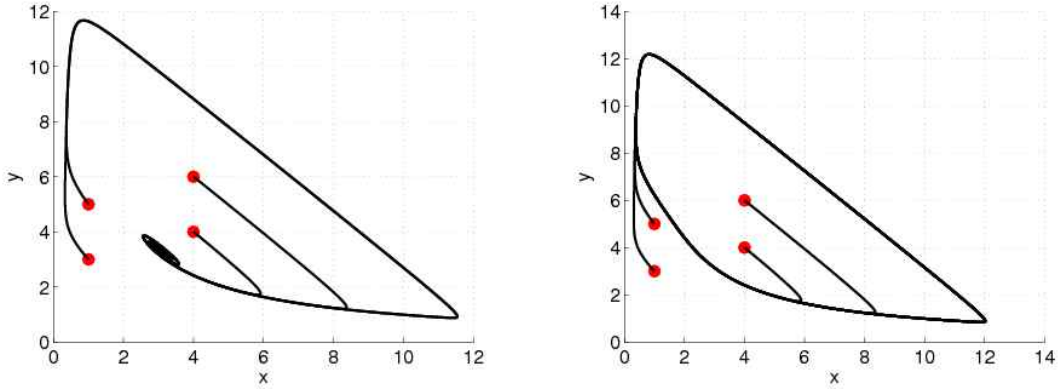

(a) $A = 3.05, B = 10$ (b) $A = 2.90, B = 10$

Figure 6.7: Orbits of the Brusselator close to the Hopf bifurcation for $B = 10, A = 3$

has the equilibrium point $(x_0, y_0) = (A, \frac{B}{A})$ with Jacobian

$$J := \begin{pmatrix} B-1 & A^2 \\ -B & -A^2 \end{pmatrix}$$

with $det(J) = A^2 > 0$. Hence $Trace(J) = 0$, i.e. $B - 1 - A^2 = 0$ is the Hopf condition. Since $A > 0$, we have $A = \sqrt{B-1}$ and $B > 1$. For $A > \sqrt{B-1}$ the equilibrium point is asymptotically stable. For $B = 10$, at $A_H := 3$ there is a supercritical Hopf bifurcation (for parameter A). See figure 6.6 and 6.7 where integral curves are shown for $A < A_H = 3$. For $A = 2.9$ one can see how the periodic solutions become pulse solutions. For $A > A_H = 3$ we see a stable focus.

6.5 Neimark-Sacker bifurcation, torus bifurcation

Let x_0 be non-degenerate fixed point of a map F for the parameter $\lambda = \lambda_0$, i.e. $1 \notin \sigma(F_x(x_0, \lambda_0))$. Then, locally there is a branch $\mathcal{C} = \{(x(\lambda), \lambda) : \lambda \in \Lambda\}$ of fixed points $x(\lambda)$ with $x(\lambda_0) = x_0$. We assume that x_0 is non-hyperbolic due to a pair of non-real, algebraically simple eigenvalues $\mu_{1,2}$ of

$F_x(x_0, \lambda_0)$ with modulus 1. Hence $\mu_{1,2} = e^{\pm i\vartheta}$ with $\vartheta \in (0, \pi)$ (**eigenvalue condition**). Then there is an open interval Λ containing λ_0, such that there are algebraically simple eigenvalues

$$\mu(\lambda) := r(\lambda)e^{\pm i\varphi(\lambda)} \in \sigma(F_x(x(\lambda), \lambda)), \quad \lambda \in \Lambda$$

with continuously-differentiable $r(\lambda)$ and $\varphi(\lambda)$ satisfying

$$r(\lambda_0) = 1, \quad \varphi(\lambda_0) = \vartheta.$$

Definition 6.7. *Under these assumptions, x_0 (or (x_0, λ_0)) is called* **Neimark-Sacker bifurcation point** *(or Hopf bifurcation point of second type) for the map F at the parameter $\lambda = \lambda_0$, if additionally the eigenvalue transversality condition $r'(\lambda_0) \neq 0$ holds.*

Theorem 6.8. *Let (x_0, λ_0) be a Neimark-Sacker bifurcation point and assume that the eigenvalue $e^{i\vartheta}$ is no first, second, third or fourth root of unity (resonance condition).*
Then, in a neighborhood of x_0, there is a branch of invariant, closed curves (cycles) for parameters λ close to λ_0. There is a parametrization of this branch by $s \in I = [0, \varepsilon), \varepsilon > 0$, such that for $s = 0$ the invariant curves shrinks to the point x_0.

Do you recognize the similarity to a Hopf bifurcation? But observe that the invariant curve *appears* as a continuous object (a curve) only after a large number of iterations.
One has to distinguish again **supercritical** and **subcritical** bifurcations, depending on the stability of the invariant curves.
See Guckenheimer–Holmes, p.162, or Wiggins, p.381 for $n = 2$. The proof can be found in Marsden–McCracken.

Example (Delayed logistic map):

$$F : \mathbb{R}^3 \to \mathbb{R}^2, \quad F(x, y, a) = (y, ay(1 - x))$$

has a supercritical Neimark-Sacker bifurcation for $a = a_0 = 2$ and $x_0 = (0.5, 0.5)$ (s. Guckenheimer–Holmes, S.163f). The eigenvalue $e^{i\vartheta}$ is the sixth root of unity.
Figure 6.8 shows invariant cycles for different values of $a > a_0$.
These pictures are taken from my Java-applet Invariant Curves.
Invariant curves of maps are much more complex objects than periodic orbits of ODEs. Bifurcation of invariant curves with respect to parameters are difficult to analyze. One example is the **phase-locking** phenomenon which has been studied by Arnold for so called standard maps (*Arnold tongues*). For our delayed-logistic-map model it occurs for $a = 2.1764$ with period and persists until $a = 2.2$.

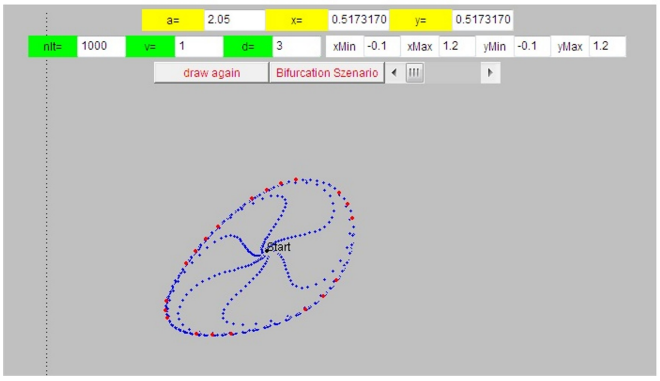

(a) $a = 2.05$

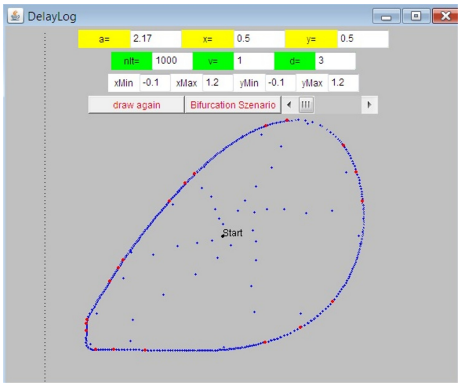

(b) $a = 2.17$

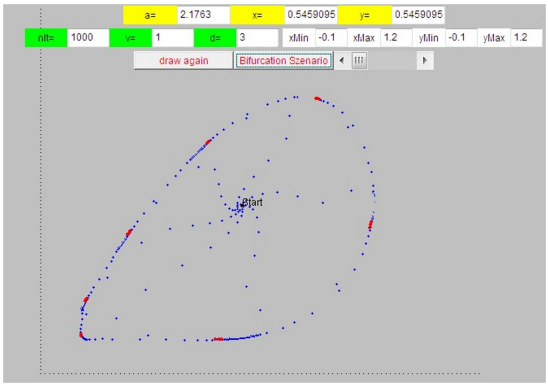

(c) $a = 2.1763$

Figure 6.8: Delayed Logistic map for different values of a

Chapter 7

Numerical bifurcation analysis

7.1 Path following

See G. Allgower, K. Georg [AG90].
Aim: Determine $\mathcal{C} := f^{-1}(0)$, where $f : D \subset \mathbb{R}^{n+1} \to \mathbb{R}^n$ is sufficiently smooth, at least continuously-differentiable.
One would expect, that all solutions of the underdetermined nonlinear system $f(x) = 0$ form one ore more (implicitely defined) curves in space.

7.1.1 Theorem of Sard

Theorem 7.1 (Sard)**.** *Let be $f \in C^\infty(D, \mathbb{R}^n)$. Then $f^{-1}(z) := \{y : f(y) = z\}$ is empty or a differentiable one-dimensional manifold for almost all $z \in \mathbb{R}^n$.*
Another formulation: Almost all $z \in \mathbb{R}^n$ are **regular values** *of f in the sense that all solutions x of $f(x) = z$ are* **regular points** *of f.*

Definition 7.2. *$y \in \mathbb{R}^{n+1}$ is called a* **regular point** *of f iff $Rank Df(y) = n$.*

IFT implies

Theorem 7.3. *Let $y_0 \in D$ be a regular point of f and $z_0 := f(y_0)$. Then there is a neighborhood $U := U(y_0)$, such that $U \cap f^{-1}(z_0)$ is a curve $\mathcal{C} := \{y(s) : |s| < \varepsilon\}$ with $y(0) = y_0$ and $y'(s) \neq 0$.*
As parameter s can be chosen any $s := y_j - y_{0,j}, j = 1, 2, ..., n+1$ for which the Jacobian $Df(y_0)$ after canceling of the jth column is a regular quadratic matrix.

In the sequel we will assume that all zeros of f are regular and that (at least a component of) $\mathcal{C} = f^{-1}(0)$ is a smooth curve.

For parameter-dependent dynamical systems this assumption implies that we expect folds, but no other complicated singularity.

The main ingredients of a path-following algorithm consists of a **predictor step**, a **corrector step** and a step size control. A posteriori a graphical presentation of the space curve $\mathcal{C}$ will be produced. For parameter dependent dynamical systems there will be one distinguished parameter, which we mainly call λ. This λ will be used for the horizontal axis of such picture, being called **solution diagram**.

7.1.2 Parametrizations of the implicitely defined curves

Differentiation of $f(y(s)) \equiv 0$ yields

Theorem 7.4. *Let be $f(y_0) = 0$, e.g. $y_0 \in \mathcal{C}$. Then the one-dimensional kernel of $Df(y_0)$ is tangential space of $\mathcal{C}$ in y_0.*

$\mathcal{C}$ needs an orientation, e.g. we have to select some direction in the one-dimensional tangen space.

Lemma 7.5. *Le $A \in \mathbb{R}^{n,n+1}$ be of (maximal) rank n. Then there is a unique $T(A) \in \mathbb{R}^{n+1}$ satisfying*

$$A \cdot T(A) = 0, \quad \|T(A)\|_2 = 1, \quad det \begin{pmatrix} A \\ T(A)^t \end{pmatrix} > 0. \tag{7.1}$$

Remark: The parameter $s := y_j - y_{0,j}$ in Theorem 7.3 can be also characterized by $T_j(y_0) \neq 0$. It seems reasonable to choose that j for which $|T_j(y_0)|$ is maximal.
Numerically there should be used an efficient algorithm for the computation of $T(A)$.

7.1.3 Folds

The two fold-conditions in Ch. 6.3 can now formulated as follows. $y_0 := (x_0, \lambda_0)$ is a regular point of f with $T(y_0) = (\varphi_0, 0)$ and $\varphi_0 \in \text{Kernel}(f_x^0)$. The last (λ)–component of y cannot been used as a suitable parameter.

Study $f(x, \lambda) = x^m - \lambda$ $(n = 1)$ and $y_0 = (0, 0)$.

7.2 Predictor– and corrector steps

We start with a given $y_0 \in \mathcal{C}$ and some desired orientation of $\mathcal{C}$, for instance increasing λ.

7.2.1 Predictor

Simplest choice: *Eulerschritt*

$$y^p := y_0 + h \cdot T(y_0)$$

with a **predictor stepsize** h.

7.2.2 Corrector

Set $y^0 := y^p$. The $(k+1)$th corrector step computes y^{k+1} by *one* Newton step for the $(n+1)\times(n+1)$–system

$$f(y) = 0, \quad a(y) = 0$$

starting with y^k. The additional real equation $a(y) = 0$ determines the corrector direction to $\mathcal{C}$ fest (and may depend on k).

a) $a(y) = y_j - y_j^p$ for a suitable j.

b) $a(y) := T(y^k)^t(y - y^k)$.
Set $A := Df(y^k)$ and

$$B := \begin{pmatrix} A \\ T(A)^t \end{pmatrix}, \quad b := \begin{pmatrix} f(y^k) \\ 0 \end{pmatrix}.$$

Solve $B \cdot dy = b$ and set $y^{k+1} := y^k - dy$.
Using a pseudo-inverse notation:

$$y^{k+1} = y^k - Df(y^k)^+ f(y^k), k = 0, 1, 2, ...$$

We need a stop condition, for instance
$\|f(y^{k+1})\| < \varepsilon$.

7.2.3 Step size control

If the corrector step is not successful, one could perform a new predictor step by halving the step size. Furthermore one needs a minimal and a maximal step size.

7.3 Further numerical comments

Willy Govaerts [Gov00].

- Equilibrium points of ODEs and fixed points of maps can be determined by Newton-like methods
- Periodic orbits or periodic solutions can be determined either by fixed point methods or by operator equations for 2π-periodic functions (as in the famous AUTO-software, Doedel et al. [DPC+01])
- Bifurcation points can be determined by so called *defining equations* which contain the equations for equilibrium points or fixed points and additionally one or more equations which characterize the special singularity. During pathfollowing it is necessary to detect bifurcation points.

Chapter 8

Microscopic traffic models

8.1 The basic model

We will consider a microscopic car-following model, where N cars are moving along a circular road of length L, i.e. we have imposed periodic boundary conditions for the traffic model on a straight line as described in Ch. 1.2. The dynamics is much richer if we make these assumptions (as in our papers [GSW04], [SGW09], [GW10]).
Let $x_j(t) \in \mathbb{R}$ be the length car No. j has covered at time t. Assume that $x_1(t) < x_2(t) < \cdots < x_N(t)$ (no overtaking) and that $x_N(t) - x_1(t) < L$.
We assume that the driver of car No. j aims for some optimal velocity depending on its headway $y_j := x_{j+1} - x_j$ according to

$$\ddot{x}_j = \frac{1}{\tau_j}(V_j(x_{j+1} - x_j) - \dot{x}_j), \quad j = 1, \ldots, N-1. \tag{8.1}$$

Here V_j is an optimal velocity function for car No. j, see below, and $\tau_j > 0$ are certain relaxation parameters which model the reaction time. For this model (8.1), the leading car dynamics must be prescribed.
The dynamics is much richer if we assume periodic boundary conditions, i.e. we have a circular road (as in our papers [GSW04], [SGW09], [GW10].)

$$\ddot{x}_j = \frac{1}{\tau_j}(V_j(x_{j+1} - x_j) - \dot{x}_j), \quad j = 1, \ldots, N, \quad x_{N+1} = x_1 + L. \tag{8.2}$$

These ODE-systems are similar to a system modeling N vibrating mass points. It is standard to write these systems as a first-order system:

$$\left\{ \begin{array}{l} \dot{x}_j = v_j, \\ \dot{v}_j = \frac{1}{\tau_j}(V_j(x_{j+1} - x_j) - v_j) \end{array} \right\}, \quad j = 1, \ldots, N, \quad x_{N+1} = x_1 + L. \tag{8.3}$$

Most numerical experiments were done for the case of identical drivers (cars):

$$\left\{ \begin{array}{l} \dot{x}_j = v_j, \\ \dot{v}_j = \frac{1}{\tau}(V(x_{j+1} - x_j) - v_j) \end{array} \right\}, \quad j = 1, \ldots, N, \quad x_{N+1} = x_1 + L. \tag{8.4}$$

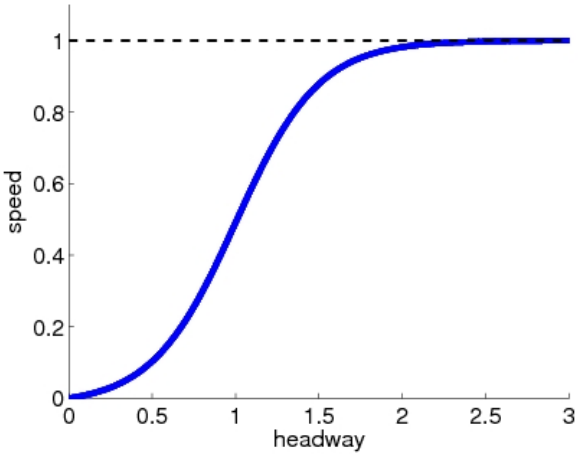

Figure 8.1: An example of an optimal velocity function (Bando, $a = 2, v_{max} = 1$)

8.1.1 Optimal velocity function

The optimal velocity function expresses the velocity the j-th car is aiming to achieve, according to the distance to the car in front. This function is assumed to be

$$\begin{aligned} V_j : [0,\infty) &\to [0,\infty), \qquad \text{smooth and strictly monotone increasing} \\ V_j(0) &= 0, \\ \lim_{d_j \to \infty} V_j(d_j) &= V_{j,max}. \end{aligned} \tag{8.5}$$

An example is given in figure 8.1.
A possible choice is

$$V(y) = v_{max} \frac{\tanh a(y-1) + \tanh a}{1 + \tanh a} \tag{8.6}$$

suggested by Bando [BHN+95]. The parameter $a > 0$ controls the steepness of V.
Another choice was suggested by Mahnke [MP97]

$$V(y) := v_{max} \frac{y^2}{a^2 + y^2}. \tag{8.7}$$

In both cases v_{max} is the maximal velocity the car would drive without a car ahead.

8.1.2 Bottleneck

The papers [SGW09], [GW10] deal with bottleneck like road works. It was introduced by extending the optimal velocity function to

$$V_{j,\epsilon}(\xi, y) = \left(1 - \epsilon e^{-(\xi - \frac{L}{2})^2}\right) V_j(y), \tag{8.8}$$

where $\varepsilon > 0$ determines the strength of the bottleneck which is centered at $L/2$ and decreases according to a Gaussian density. Now the optimal velocity function does also depend on the position ξ on the circular road by reducing the maximal velocity $v_{j,max}$ to

$$v_{j,max}(\xi) = v_{j,max} \cdot \left(1 - \epsilon e^{-(\xi - \frac{L}{2})^2}\right).$$

Our general ODE system now reads as

$$\ddot{x}_j = \frac{1}{\tau_j}\left(V_{j,\varepsilon}(\xi_j, x_{j+1} - x_j) - v_j\right), \quad j = 1, \ldots, N, \quad x_{N+1} = x_1 + L. \tag{8.9}$$

where the (position) variables ξ_j are defined by

$$0 \le \xi_j \le L, \qquad \xi_j = x_j \bmod L. \tag{8.10}$$

.

We will mainly study the dynamics in dependence ob N, L and ε by fixing $\tau_j, v_{j,max}$ and a_j. Observe that $\frac{N}{L}$ is the average density on the circular road.

8.1.3 Some extension of the model

Up to now only the headway to the car in front determines the velocity a driver is aiming to achieve. It could be more realistic that also the differences of the velocities has some influence. This leads to the model

$$\ddot{x}_j = \frac{1}{\tau_j}\Big(V_j(x_{j+1} - x_j) - \dot{x}_j\Big) + g_j(x_{j+1} - x_j) \cdot (\dot{x}_{j+1} - \dot{x}_j), j = 1, ..., N, x_{N+1} = x_1 + L, \tag{8.11}$$

where g_j is a function of the headways, called *aggressiveness term*. In the case of identical drivers there is only one function $g = g_j$ and (8.11) becomes

$$\ddot{x}_j = \frac{1}{\tau}\Big(V(x_{j+1} - x_j) - \dot{x}_j\Big) + g(x_{j+1} - x_j)(\dot{x}_{j+1} - \dot{x}_j), j = 1, ..., N, x_{N+1} = x_1 + L. \tag{8.12}$$

respectively

$$\begin{array}{rcl} \dot{x}_j &=& v_j \\ \dot{v}_j &=& \frac{1}{\tau_j}\Big(V_j(x_{j+1} - x_j) - v_j\Big) + g_j(x_{j+1} - x_j)(v_{j+1} - v_j) \end{array} \tag{8.13}$$

8.1.4 Quasi-stationary solutions

The simplest solutions for the bottleneck-free case are those, where all cars have the same speed c and constant headways $d_j := x^0_{j+1}(t) - x^0_j(t) > 0, j = 1, 2, ..., N$. These solutions are called **quasi-stationary**. It is simple to prove that there is a unique quasi-stationary solution: The unknown headways d_j and the unknown speed c have to satisfy

$$c = V_j(d_j), j = 1, 2, ..., N, \quad \sum_{j=1}^{N} d_j = L.$$

For each c smaller than the smallest maximal velocity $v_{min,max}$ of all cars there are unique, continuous, monotone increasing functions $d_j(c)$. For at least one j we have $d_j(c) \to \infty$ for $c \to v_{min,max}$.
For identical drivers the quasi-stationary solutions are very simple: All headways equal L/N and the common speed c satisfies $c = V(L/N)$.
Our first result is concerned with the stability of the quasi-stationary solutions and the loss of their stability by variation of the density L/N. The analysis can be performed for identical cars. For more general cases only numerical analysis would help.

8.1.5 Stability of the quasi-stationary solutions

Introduce headways $y_j := x_{j+1} - x_j$ instead of x_j and leave the speeds v_j as they are ($j = 1, 2, ...N$). In these new coordinates our general first order-system (8.13) becomes

$$\left\{ \begin{array}{lcl} \dot{y}_j & = & v_{j+1} - v_j \\ \dot{v}_j & = & \frac{1}{\tau_j}\Big(V_j(y_j) - v_j\Big) + g_j(y_j)(v_{j+1} - v_j) \end{array} \right\} \quad j = 1, \ldots, N, \quad v_{N+1} = v_1 \tag{8.14}$$

Set $\mathbf{x} := (y_1, ..., y_N, v_1, ..., v_N)$ and let $f(\mathbf{x})$ be the right hand side of (8.14). Then $\mathbf{x}_0 := (d_1, ..., d_N, c, ..., c)$ is an equilibrium point, and the Jacobian $A := Df(\mathbf{x}_0)$ is given by

$$A = \begin{pmatrix} & & & -1 & 1 & & & \\ & & & & \ddots & \ddots & & \\ & & & & & -1 & 1 & \\ & & & 1 & & & -1 & \\ \beta_1 & & & (-\frac{1}{\tau_1} + \gamma_1) & -\gamma_1 & & & \\ & \ddots & & & \ddots & \ddots & & \\ & & \beta_{N-1} & & & (-\frac{1}{\tau_{N-1}} + \gamma_{N-1}) & -\gamma_{N-1} & \\ & & & \beta_N & -\gamma_N & & (-\frac{1}{\tau_N} + \gamma_N) & \end{pmatrix},$$

where $\beta_j := \frac{1}{\tau_j} V_j'(d_j)$, $\gamma_j := g_j(d_j)$.
Using the ordering $\mathbf{x} := (y_1, v_1, ..., y_N, v_N)$ and the 2×2-matrices

$$D_j := \begin{pmatrix} 0 & -1 \\ \beta_j & -\frac{1}{\tau_j} - \gamma_j \end{pmatrix}, \; j = 1, ..., N, \quad \mathcal{N}_j := \begin{pmatrix} 0 & 1 \\ 0 & \gamma_j \end{pmatrix}$$

A turns out to be a block-cyclic matrix with diagonal blocks D_j and off-diagonal blocks $\mathcal{N}_j$:

$$A = \begin{pmatrix} D_1 & \mathcal{N}_1 & O & \ldots & O \\ O & D_2 & \mathcal{N}_2 & \ldots & O \\ \vdots & \ddots & \ddots & \ddots & \vdots \\ O & \ldots & O & D_{N-1} & \mathcal{N}_{N-1} \\ \mathcal{N}_N & \ldots & \ldots & O & D_N \end{pmatrix}$$

With different methods one can show that

$$\chi_A(\lambda) = \Big(\lambda(\lambda + \frac{1}{\tau_1}) + \beta_1\Big) \cdots \Big(\lambda(\lambda + \frac{1}{\tau_N}) + \beta_N\Big) - \beta_1 \cdots \beta_N, \tag{8.15}$$

for the characteristic polynomial without aggressiveness, which simplifies in the case of identical cars

$$\chi_A(\lambda) = \Big(\lambda(\lambda + \frac{1}{\tau}) + \beta\Big)^N - \beta^N. \tag{8.16}$$

(see Theorem 8.1).
We state for the general case with aggressiveness

Theorem 8.1. *The eigenvalues λ of the Jacobian A are solutions of the polynomial equation*

$$\prod_{j=1}^{N} \Big(\lambda(\lambda + \gamma_j + \frac{1}{\tau_j}) + \beta_j\Big) = \prod_{j=1}^{N} (\gamma_j\lambda + \beta_j). \tag{8.17}$$

For identical cars the equations simplifies to

$$\Big(\lambda(\lambda + \gamma + \frac{1}{\tau}) + \beta\Big)^N = (\gamma\lambda + \beta)^N. \tag{8.18}$$

There are different **proofs**. I like the following **Ansatz** which takes the cyclic structure into account: Set $u := (u_1, ..., u_N)$ with $u_j \in \mathbb{C}^2$ and $u_{j+1} = \mu_j u_j, \mu_j \in \mathbb{C}, j = 1, 2, ..., N, u_{N+1} = u_1$, for a block-eigenvector of A for the eigenvalue λ. From $u_{N+1} = u_1$ it follows that $\prod_{j=1}^N \mu_j = 1$.
Now the eigenvalue block-equation becomes

$$D_j u_j + \mu_j \mathcal{N}_j u_j = \lambda u_j, j = 1, 2, ..., N,$$

and λ turns out to be an eigenvalue of the 2×2-matrices $D_j + \mu_j \mathcal{N}_j, j = 1, ..., N$, and it follows that

$$\lambda(\lambda + \gamma_j + \frac{1}{\tau_j}) + \beta_j = \mu_j(\gamma_j\lambda + \beta_j)$$

which implies (8.17).
Conversely, any solution λ of (8.17) is an eigenvalue of $D_j + \mu_j \mathcal{N}_j$, where

$$\mu_j := (\lambda(\lambda + \gamma_j + \frac{1}{\tau_j}) + \beta_j)/(\gamma_j\lambda + \beta_j)$$

satisfying $\prod_{j=1}^N \mu_j = 1$. The Ansatz works. ∎

Obviously $\lambda = 0$ is an algebraically simple eigenvalue of A which prevents us to apply the principle of linearized stability. One can show that $\lambda = 0$ holds due to the first integral $H(y, v) := \sum_{j=1}^N y_j$.
The trivial eigenvalue $\lambda = 0$ can be removed, by eliminating $y_N = L - y_1 - \cdots - y_{N-1}$ from (8.2) to obtain the $(2N-1)$-System

$$\left\{ \begin{array}{lcl} \dot{y}_j & = & v_{j+1} - v_j \\ \dot{v}_j & = & \frac{1}{\tau_j}(V_j(y_j) - v_j) \\ \dot{v}_N & = & \frac{1}{\tau_N}(V_N(L - y_1 - \cdots - y_{N-1}) - v_N) \end{array} \right\}, \quad j = 1, \ldots, N-1. \tag{8.19}$$

Now the equilibrium point is $\mathbf{x}^0 := (d_1, ..., d_{N-1}, c, ..., c)$. Its Jacobian has the same eigenvalues except $\lambda = 0$.

8.1.6 Eigenvalue analysis

We investigate the eigenvalue equation for identical cars without aggressiveness and $\tau = 1$. Hence an eigenvalue of the Jacobian A satisfies

$$(\lambda^2 + \lambda + \beta)^N = \beta^N, \beta := V'(L/N) > 0.$$

Hence $z := \frac{\lambda^2+\lambda+\beta}{\beta}$ is an Nth root of unity $z = c_k + is_k$ with $c_k := \cos(2\pi k/N), s_k := sin(2\pi k/N)$ where $k = 1, 2, ..., N$. We call an eigenvalue λ with $\frac{\lambda^2+\lambda+\beta}{\beta} = c_k + is_k$ an eigenvalue of *type k*. Since $\lambda^2 + \lambda$ is invariant under the reflection $\lambda \mapsto -(\lambda + 1)$ (at $x = -\frac{1}{2}$), the two eigenvalues of the same type are symmetric wrt $x = -\frac{1}{2}$. For $k = N$ we have the two eigenvalues $\lambda = 0$ and $\lambda = -1$ (for all β). All other eigenvalues are non-real except for even N and $k = N/2$ (for β large enough).
The four eigenvalues of type k and of type $N - k$ (for $k \neq N/2$) form two pairs of conjugate complex numbers.
We are interested in the dependence of the eigenvalues on $\beta = V'(L/N)$. Observe that the optimal velocity functions V have small $V'(y) > 0$ for small and for large y. We will see that for small β all eigenvalues except our black sheep $\lambda = 0$ are lying in the left half of the complex plane, but that for increasing β complex conjugate pairs (of type k and $N-k$) will cross the imaginary axis with non-zero speed. This occurs for

$$\beta = \beta_k := \frac{1}{1 + \cos(2k\pi/N)}. \tag{8.20}$$

Taking β as bifurcation parameter, we have h_N Hopf bifurcations with $h_N := (N - 1)/2$ for odd N and $h_N := N/2 - 1$ for even N. The corresponding imaginary eigenvalues are $i\omega_k$ with

$$\omega_k = \frac{s_k}{1 + c_k},$$

see [GSW04].
The first Hopf-pair of eigenvalues, where the stability is lost, is that of type 1 and of type $N - 1$ when

$$\beta = \frac{1}{1 + \cos(2\pi/N)}. \tag{8.21}$$

Hence we have the **Hopf condition**

$$V'(L/N) = \frac{1}{1 + \cos(2\pi/N)}. \tag{8.22}$$

It can be easily seen that this **Hopf equation** has in general no solution or two solutions, in an exceptional case one double solution. This depends on v_{max} in the Bando- or Mahnke function. Assuming that v_{max} is large enough there are two **Hopf-lengths** $0 < L_1^H < L_2^H$ or two **Hopf headways** $0 < y_1^H < y_2^H, y_j^H := L_j^H/N$ satisfying

$$V'(L_j^H/N) = \frac{1}{1 + \cos(2\pi/N)}, j = 1, 2,$$

see figure 8.2 for large N when the Hopf equation becomes $V'(L/N) = \frac{1}{2}$.

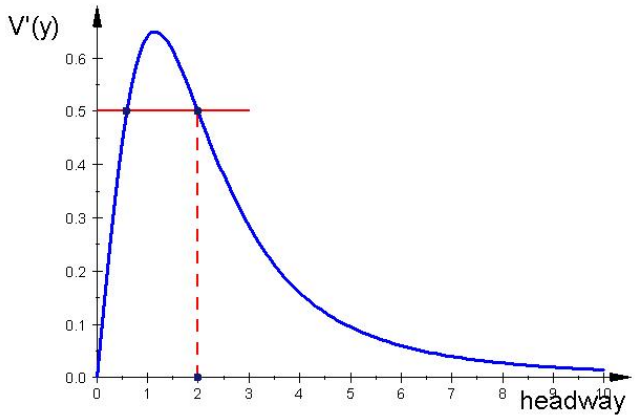

Figure 8.2: Hopf headways

The Hopf-periodic solutions satisfy some symmetry condition, due to the fact the we have identical drivers. Therefore, having any periodic solution, we get another one by a forward numbering shift

$$S_+(x_1, ..., x_N, v_1, ..., v_N) := (x_2, x_3, ..., x_N, x_1 + L, v_2, v_3, ..., v_N, v_1) \tag{8.23}$$

of the car constellation on the circle. In the Hopf bifurcation Theorem the bifurcation periodic orbits are unique. Hence the shift S_+ maps the periodic orbit on itself. This leads the the property

$$v_j(t + T/N) = v_{j+1}(t) \text{ for all } t, \quad j = 1, 2, ..., N, \tag{8.24}$$

for the velocities and analogously for the headways. As a consequence, a projection of the periodic orbit onto the headway-speed plane of any car yields the same result, see figure 8.6(c).
The quasi-stationary solutions are stable for $L < L_1^H$ (slow traffic speed with high density) and for $L > L_2^H$ (fast traffic speed with low density). Most interesting is the larger Hopf length L_2^H (the larger Hopf headway, the smaller Hopf density), it determines the critical density when the quasi-stationary solution looses its stability.

Figure 8.4 shows a solution diagram with stable and unstable quasi-stationary solutions and stable periodic solutions.

8.1.7 Traffic flow

Physically the flow is speed times density. It measures the number of cars passing the road per time unit.
For the microscopic model the reciprocal of the headway is a good substitute of density. Hence the traffic flow of a quasi-stationary solution is given by $f = V(L/N) \cdot N/L$, for a given headway y we have $f = V(y)/y$. Or setting $\varrho = \frac{1}{y}$ we have $f = f(\varrho) := \varrho \cdot V(1/\varrho)$, see figure 8.3 for quasi-stationary solutions.
The two Hopf headways correspond with two Hopf densities. We are mostly interested in the smaller Hopf density.
Question: Is the quasi-stationary solution with maximal traffic flow (for density ϱ_m) stable? Where are the Hopf densities located? There are no general answers.

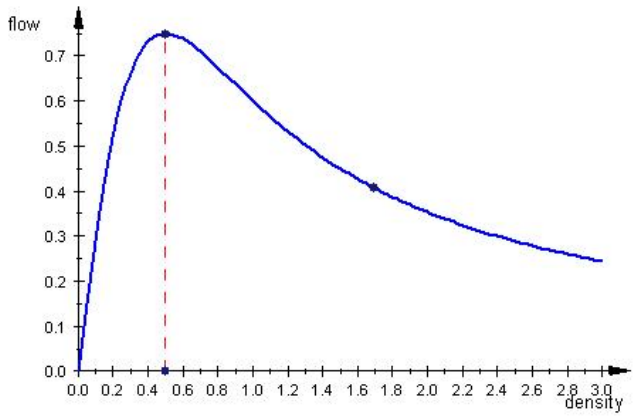

Figure 8.3: Traffic flow as function of the density

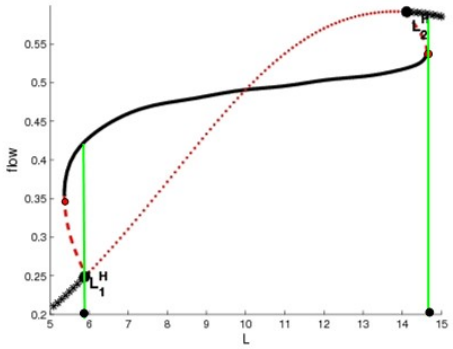

Figure 8.4: Solution Diagram Hopf-periodic solutions $N = 10$

8.1.8 Some computations and simulations for the bottleneck-free case

As in [GW10] we restrict our attention to $N = 10, \tau = 1$ and to the Bando optimal velocity function

$$V(y) = v_{max} \frac{\tanh a(y-1) + \tanh a}{1 + \tanh a} \tag{8.25}$$

with $a = 2, v_{max} = 1$.
Then we compute

$$0 < L_1^H = 5.89 < L_2^H = 14.109, 0 < y_1^H = 0.589 < y_2^H = 1.4109, 0 < \varrho_2^H = 0.7088 < \varrho_1^H = 1.698.$$

The flow for $\varrho = \varrho_2^H = 0.7088$ is almost maximal ($f = 0.591$), its speed is also almost maximal $=0.9839$. The Hopf bifurcation at $L_2^H = 14.109$ appears to be extremely subcritical: Stable periodic solutions live for $L = 14.6$ and coexist with stable quasi-stationary solutions. For $L = 14.7$ they die, only the stable quasi-stationary solutions survive. Figure 8.7 for $L = 14.6$ and figure 8.6 for $L = 14.1$

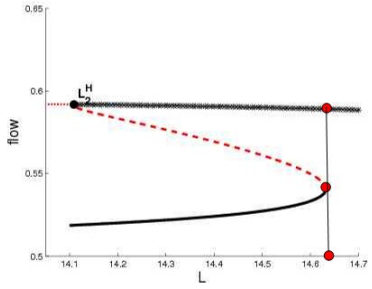

Figure 8.5: Solution Diagram Detail from figure 8.4

show the stable periodic solutions which are heavily congestive with a traveling wave structure. There is a very "hard" transition from the "nice" quasi-stationary solutions to very congestive traveling wave solutions.

But the subcriticality of the Hopf bifurcation which seems to be obvious from figure 8.4 and particularly from figure 8.5, contradicts the result in [SGW09] where for the Bando function it is shown that the Hopf bifurcations are always supercritical. Indeed, we found for $L = 14.10 < L_2^H = 14.109$ stable periodic orbits with a very small amplitude without any dramatic jam structure (see figure 8.8) which coexists with the "dramatic" traveling wave solution in figure 8.6. But already for $L = 14.05$ they have lost their stability, and the only stable dynamics is given by the traveling waves. It might be interesting that the global flows of the qualitatively very different dynamics are almost the same.

Numerically, the almost invisible supercriticality of the Hopf bifurcation can be seen from figure 8.9 which presents a very small detail of figure 8.4.

The other Hopf bifurcation at $L_1^H = 5.89$ seems also to be "macroscopically" subcritical. Period orbits exist until $L = 5.4$. But also this Hopf bifurcation is "microscopically" supercritical.

This example shows that the Lyapunov coefficient the sign of which determines the sub (super-) criticality may mislead the analysis.

8.2 Bottlenecks

We revisit the model in Ch. 8.1.2.

In the bottleneck-free case all positions $\xi \in S_1^L$ were equal, the space-period L was not really important. The periods of the Hopf-periodic solutions were not determined by L. The situation was mathematically very special since the quasi-stationary solutions formed a stationary point in the system for the relative velocities and the headways. Therefore standard methods for the stability analysis of stationary points of autonomous ODE systems could be applied. In the more general case with bottleneck the situation is different since we do not know what the generalization of a quasi-stationary solution is. Rewriting the system in terms of relative velocities and headways does not show any advantage since there are no interesting stationary points. Therefore in this case a completely different approach has to be used. It turns out that so-called rotation solutions are the right object to look for (see [SGW09]).

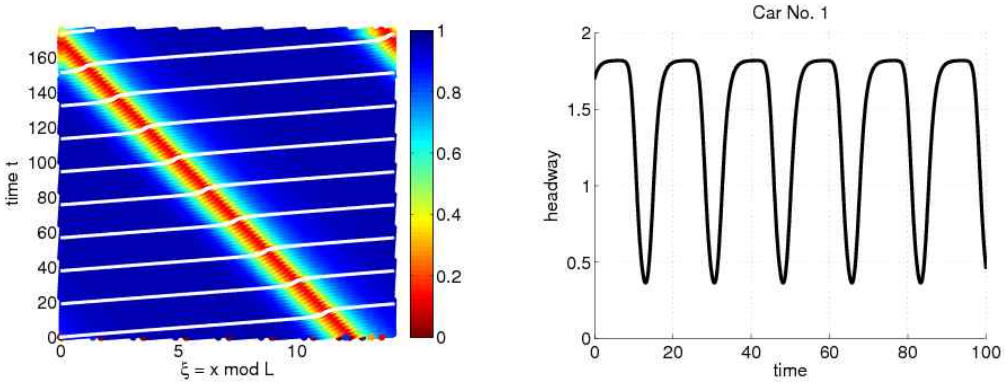

(a) Macro

(b) Time-headway

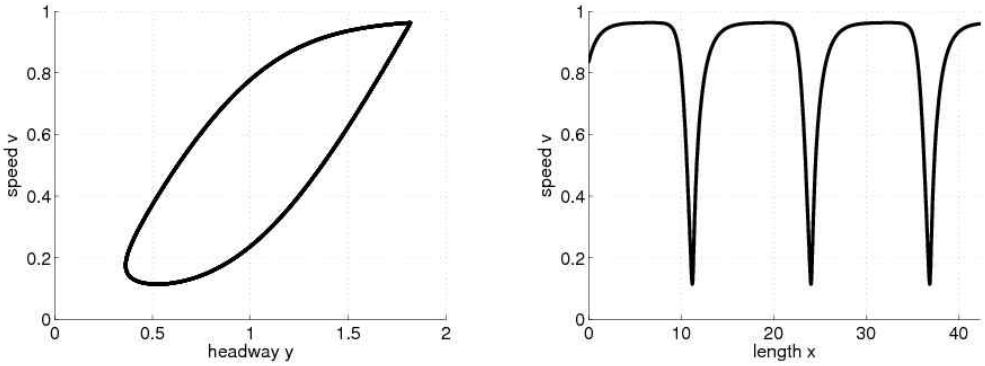

(c) Phase curve headway-speed

(d) Length-speed

Figure 8.6: Hopf-periodic orbit $N = 10, L = 14.1 < L_2^H, \varepsilon = 0$

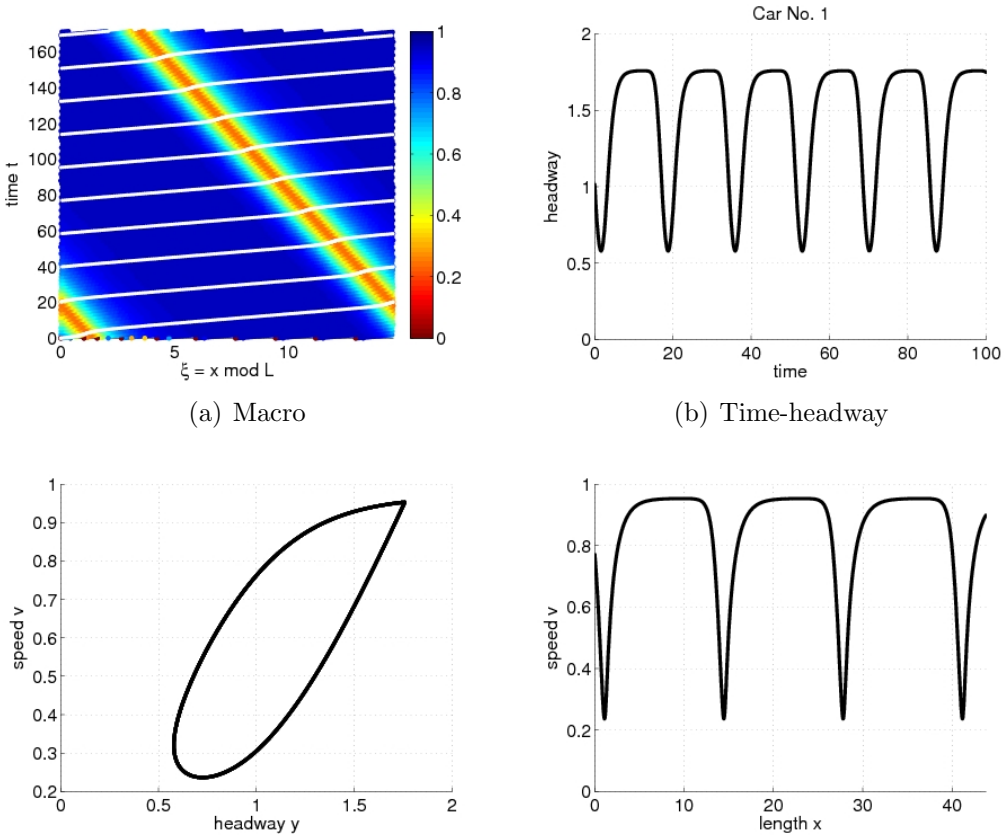

(a) Macro

(b) Time-headway

(c) Phase curve headway-speed

(d) Length-speed

Figure 8.7: Hopf-periodic orbit $N = 10, L = 14.6 > L_2^H, \varepsilon = 0$

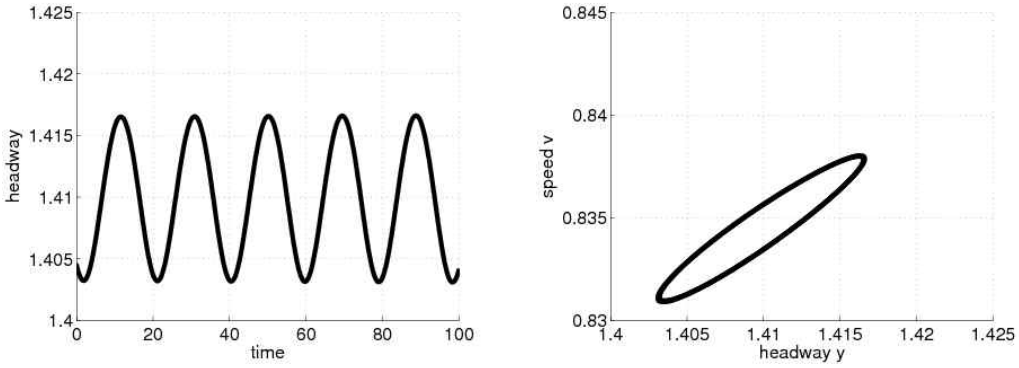

(a) Time-headway

(b) Phase curve headway-speed

Figure 8.8: Hopf-periodic orbit $N = 10, L = 14.1 < L_2^H = 14.109, \varepsilon = 0$

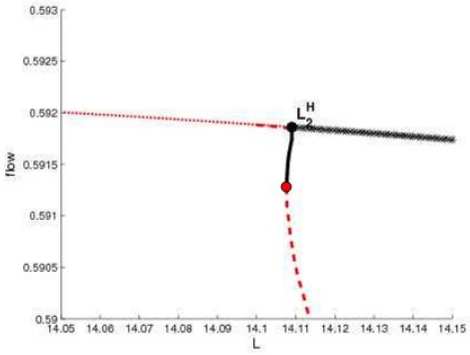

Figure 8.9: A detail of figure 8.4

8.2.1 Rotation solutions

A **rotation solution** with **orbital period** T is defined by

$$x_j(t+T) = x_j(t) + L, \quad v_j(t+T) = v_j(t), \qquad j = 1, 2, ..., N, \tag{8.26}$$

where T is assumed to be minimal. From a traffic point of view a rotation solution is nothing but a standing wave for the velocity or the headways (see figure 8.12). Mathematically it is a T-periodic solution on the manifold $(S_1^L)^N \times \mathbb{R}^N$.
We see that for $\varepsilon = 0$, our quasi-stationary solutions are (trivial) rotation solutions with *orbital period* $T := L/v^0$, where v^0 is the common velocity of the drivers. But observe that the Hopf-periodic solutions (traveling waves) in general are *not* rotation solutions with orbital period T. They always satisfy

$$x_j(t+T) = x_j(t) + L_p, j = 1, 2, ..., N \tag{8.27}$$

with an orbital length L_p.
Again, the question whether a solution can be observed in real traffic situations or in experiments is related to the stability of the solution. The corresponding stability concept for rotation solutions was discussed in [SGW09]. The (orbital) stability concept is that of periodic orbits of autonomous ODEs, the only technical problem (which is also relevant when we apply numerical methods) is that we deal with a manifold instead of the simple Euclidian space $\mathbb{R}^n$. Hence we know that we should apply something like Poincaré maps for suitable transversal sections to get the Floquet multipliers of the rotation solutions.

Therefore we rewrite our problem in a fixed point problem.
The time-T-map Φ^T is defined as follows: Assume that $\mathbf{x}(0) = (x_1, ..., x_N, v_1, ..., v_N)$ is the state of our system at time $t = 0$ and that $\mathbf{x}(t)$ is the solution of the corresponding initial value problem. Then

$$\Phi^T(\mathbf{x}(0)) = \mathbf{x}(T). \tag{8.28}$$

Setting $\Lambda := (L, ..., L, 0, ..., 0)$, rotation solutions satisfy (rewriting (8.26))

$$\Phi^T(\mathbf{x}(t)) = \mathbf{x}(t+T) = \mathbf{x}(t) + \Lambda \text{ for all } t. \tag{8.29}$$

Therefore, rotation solutions are fixed points of the map Q defined by

$$Q(\mathbf{x}) = \Phi^T(\mathbf{x}) - \Lambda. \tag{8.30}$$

This means that in case of bottleneck instead of quasi-stationary solutions we have rotation solutions solving the fixed point problem (8.30). Note that when looking for rotation solutions we do not know the period T a priori. We will not consider the map Q itself, but a related Poincaré map Π. There is a simple choice for the transversal section, given by a measure point on the circle at some point $\xi \in S_1^L$, say at $\xi = 0$. Whenever car No. 1 passes the measure point, the whole car configuration (and the discrete time of this event) are listed.

We note that – similar to the bottleneck-free case – when reaching a critical density, the rotation solutions may loose their stability. This is due to Neimark–Sacker bifurcation. In the bottleneck-free case – when passing the critical parameter values – Hopf-periodic solutions bifurcate whereas Neimark-Sacker bifurcation leads to so called quasi-rotation solutions. We will see that contrary to Hopf-periodic or rotations solutions it is not so easy to identify quasi-rotation solutions. We will see that they seem to be combinations of standing and traveling waves.
As a consequence, in the (L, ϵ)-plane we conjecture parameter regions where rotations and quasi rotations exist which at $\epsilon = 0$ coincide with the quasi-stationary solutions and the Hopf-periodic solutions, respectively. Between these two parameter regions we expect a curve on which Neimark–Sacker bifurcations take place for $\epsilon > 0$. For Hopf values L^H such a curve will emanate at $(0, L^H)$. We will intensively study different parameter regions to verify this conjecture (see figure 8.11).
In [SGW09] we showed the existence of rotation solutions for small $\varepsilon > 0$ by considering the case of a small bottleneck as a perturbation of the bottleneck-free case. (Un)stable quasi-stationary solutions are perturbed to un(stable) rotation solutions. Hopf-periodic solutions are perturbed to quasi-rotations.

8.2.2 Identical drivers with bottleneck: POMs

We restrict and simplify the setting to the case of identical drivers. This is done by adding an additional symmetry condition (see (8.24) for the Hopf-periodic solutions) to a rotation solution, namely

$$x_j(t + T/N) = x_{j+1}(t) \text{ for all } t, \quad j = 1, 2, ..., N. \tag{8.31}$$

This means that in the case of identical drivers all cars behave in the same way except a time shift of T/N between two cars. Rotation solutions satisfying (8.31) are known as Ponies-on-a-Merry-Go-Round-solutions (POMs) (see [AGMP91], [SGW09]). It turns out that the method to search rotation solutions presented in the previous Ch. 8.2.1 can be simplified considerably. The additional condition (8.31) allows the use of so-called **reduced Poincaré maps** π, and the computation of POMs can be based on π in a very efficient way. (The return time for π is the Nth fraction of that for Π.) While the Poincaré map looks for discrete times whenever the car No. 1 passes the position $\xi = 0$, the reduced Poincaré map lists the whole configuration at discrete times whenever *any* car passes the position $\xi = 0$. This gives a denser discrete time grid on which the dynamics is evaluated.
We obtain the (discrete) orbit under π as follows: Whenever any car passes $\xi = 0$, a snapshot is taken of the whole car ensemble. After this event there is a renumbering. The cars ar numbered according to the position on the circle: car No. 1 at $\xi = 0$, then car No. 2 etc.:

$$0 = \xi_1 < \xi_2 < \cdots < \xi_N < L.$$

Mathematically, POMs correspond to fixed points and quasi-POMs to invariant curves of π which bifurcate in Neimark–Sacker-points of π. Again, quasi-stationary solutions correspond to POMs and Hopf-periodic solutions to quasi-POMs for $\varepsilon = 0$.
Our numerical analysis in the following section is performed for the model of identical drivers and is based on the use of reduced Poincaré maps. More theoretical details can be found in [SGW09].

8.3 Numerical results: POMs and quasi-POMs

We consider the general model (8.9) for identical drivers,

$$\left\{ \begin{array}{rcl} \dot{x}_j & = & v_j \\ \dot{v}_j & = & \frac{1}{\tau}(V_\varepsilon(\xi_j, x_{j+1} - x_j) - v_j) \end{array} \right\}, \quad j = 1, \ldots, N, \quad x_{N+1} = x_1 + L. \tag{8.32}$$

with

$$V_\epsilon(\xi, y) = \left(1 - \epsilon e^{-(\xi - \frac{L}{2})^2}\right) V(y). \tag{8.33}$$

We restrict our attention to $N = 10, \tau = 1$ and to the Bando optimal velocity function

$$V(y) = v_{max} \frac{\tanh a(y-1) + \tanh a}{1 + \tanh a} \tag{8.34}$$

with $a = 2, v_{max} = 1$.
We know that for $\varepsilon = 0$ there exist two Hopf bifurcation points with respect to L, namely $L_1^H = 5.890$ and $L_2^H = 14.109$. The larger value L_2^H is more interesting, since it is connected with the first loss of stability of the quasi-stationary solutions for increasing traffic densities N/L. Moreover, we know that the quasi-stationary solutions (being special POMs) are unstable for $L_1^H < L < L_2^H$.
It is impossible to give a complete survey about the dynamics of the model for all parameter pairs (L, ε). We will mainly present some results for two fixed values of L, namely $L = 13 < L_2^H$ and $L = 18 > L_2^H$.

The dynamics of POMs and quasi-POMs will be visualized in three ways using suitable projections.

1. Speed of a single car as a function of length (Lagrangian description). For a POM we will encounter an L-periodic pattern (example: figure 8.12(a)).

2. Macroscopic view (Eulerian description). This is obtained by coloring all trajectories according to the speed of the corresponding car. Hereby we obtain a discrete version of the speed $v(\xi, t)$ as function of position ξ and time t. One single trajectory is drawn (example: figure 8.12(b)).

   For a POM, $v(\xi, t)$ is independent of t. For a quasi-POM we have the interesting observation that $v(\xi, t)$ is periodic in t.

3. More mathematically, the orbit under the reduced Poincaré map, mainly showing the limit set. For a POM the limit set is just a point, for a quasi-POM we will encounter closed invariant curves (example: figure 8.17(a)).

8.3.1 POMs (standing waves)

We are interested in how the POMs change with ε for fixed L. To this end we continue numerically POM-branches in dependence on (as a function of) the bottleneck strength ε using the characterization of POMs as fixed points of (reduced) Poincaré maps.
From the theory in [SGW09] we know that for fixed L, a POM-branch parametrized by $\varepsilon \geq 0$ emanates from the quasi-stationary solution ($\varepsilon = 0$). We will path follow POM-branches also for larger values of ε. Some results are visualized in figure 8.10. As expected we encounter Neimark–Sacker bifurcation points, but also – less expected – folds.

In figure 8.10 (vertical axis) a POM is characterized by the average speed $v_M := L/T$ with T being the orbital period. v_M is proportional to the space-averaged flow f. The horizontal coordinate is the bottleneck strength ε. For $\varepsilon = 0$ the trivial POM coincides with the quasi-stationary solution where all cars have the same speed $v_M = V(L/N)$. The numerical continuation is not influenced by the stability of the POMs. Of an obvious interest are those (bifurcation) parameters ε where stability is lost or gained. We encounter two qualitatively different bifurcations: Neimark-Sacker points (as in figure 8.10(a) denoted by N) and fold points (as in figure 8.10(d) denoted by F_1 and F_2).
In figure 8.10 folds can be found on the POM-branches. For $L = 18$ there are two folds for $\varepsilon_1 := 0.22$ and for $\varepsilon_2 := 0.313$, two other folds are very close together at $\varepsilon \approx 0.41$. Observe that the S-shape of the POM-branch with two neighbored folds are associated with the coexistence of two stable POMs for the same parameter set. We will see that the wave-speed of these two stable POMs in the vicinity of the bottleneck differs significantly. This is already indicated by the corresponding different average speeds.In the mentioned theory of Kerner (2008) the POMs seem to correspond to the so called congested traffic phase.

Bifurcation diagrams in L and ε

A bifurcation diagram in a parameter plane shows bifurcation curves. By this it contributes to the information about possible dynamics for a fixed pair of parameters.
In our traffic model we expect Neimark–Sacker and fold curves showing the dependence of the bifurcation parameters ε on the circle length L. Figure 8.11 contains Neimark–Sacker (red) and fold curves (black) in the (L, ε)-parameter plane. The Neimark-Sacker curve emanates in the Hopf point $(0, L_2^H)$. Though these curves deliver only local information, we guess, supported by numerical simulations, that quasi-POMs live in the red-shaded region, where POMs are unstable. In the other parameter domains we expect stable POMs. In the black-shaded areas, due to the S-shape of the POM-branches in figure 8.10, we expect two stable POMs and one unstable POM.

POMs for L=18

Figure 8.12 visualizes different stable POMs for $L = 18$ and various ε-values. They can be computed directly by Newtons method as fixed points of the reduced Poincaré maps — in contrast to the quasi-POMs which we get only by simulation, see Ch.8.3 and Ch. 8.3.2. From figure 8.10(c) we conclude, that for some values ε, the corresponding POMs are not unique. For example, there are two coexisting stable POMs and one unstable POM for $\varepsilon = 0.3$, a value between the two fold values $\varepsilon_1 = 0.22$ and

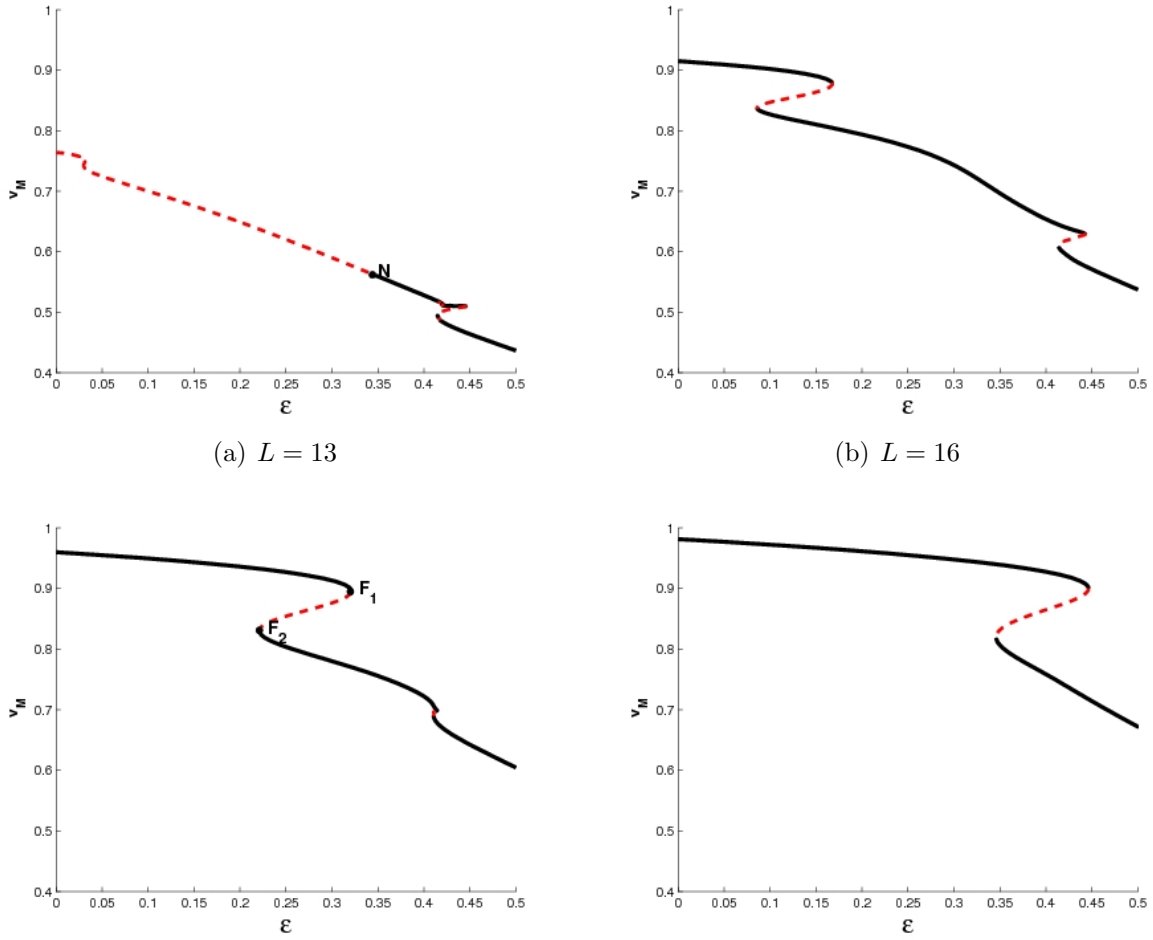

(a) $L = 13$

(b) $L = 16$

(c) $L = 18$

(d) $L = 20$

Figure 8.10: $N = 10$. Dependence of the average speed v_M of the POMs on ε for fixed L. Solid (dashed) lines: Stable (unstable) POMs. The Neimark-Sacker bifurcation in (a) is indicated by the letter N. Folds in (c) are indicated by the letters F_1 and F_2.

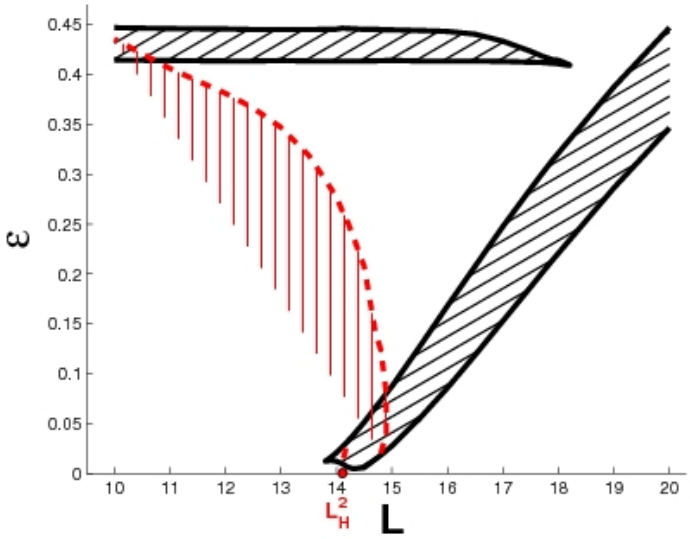

Figure 8.11: $N = 10$. Bifurcation diagram. Neimark-Sacker curve (red, dashed line), fold curves (black, solid line)

$\varepsilon_2 = 0.313$, see figures 8.12(c) - 8.12(f). These two stable POMs are qualitatively very different. This is already indicated by the difference of their average speeds v_M.
Remarkably, the decrease of speed induced by the bottleneck is considerably large only for the POMs in the last rows of figure 8.12 and figure 8.3.1. Here traffic jams occur downstream the bottleneck while for the POMs in the first two rows of figure 8.12 the minimal speed occurs upstream the bottleneck (the black circles in figure 8.12 and figure 8.3.1). For $\varepsilon = 0.3$ both types of stable POMs do exist.

8.3.2 Quasi-POMs for L=13

In this section we fix $L = 13$. We know from figure 8.11 and particularly from figure 8.10(a) that there is a wide parameter range where POMs emanating from the quasi-stationary solutions for $\varepsilon = 0$ are unstable. Here we expect quasi-POMs.
We present three different visualizations of quasi-POMs, see figures 8.14-8.17. Again each quasi-POM is associated with the average speed v_M where the average is taken over a suitable large time interval. Quasi-POMs are special solutions which show non-periodic dynamic behavior for $t \to \infty$ when considering the trajectories of individual vehicles. Theoretically, the quasi-POM type irregularity can be identified by closed invariant curves of (reduced) Poincaré maps as shown in figure 8.17. But we found another way of identification, namely the time-periodicity of the macroscopic function $v(\xi, t)$ in the macroscopic views in figures 8.14-8.16 (right side).
In figure 8.10(a) there is a Neimark–Sacker bifurcation for $\varepsilon \approx \varepsilon_N := 0.347$, and the POMs are stable for $\varepsilon > \varepsilon_N$ and unstable for $\varepsilon < \varepsilon_N$. Hence one could expect quasi-POMs for $\varepsilon < \varepsilon_N$.
Moreover, we know that for $\varepsilon = 0$ the quasi-stationary solution is unstable. The Hopf point at L_2^H is responsible for the occurrence of a stable headway- and speed-periodic solution appearing as a traveling

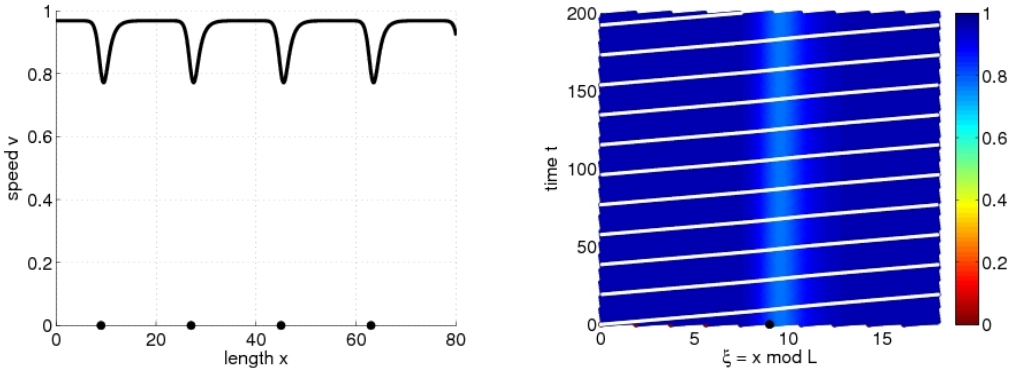

(a) $\varepsilon = 0.2, v_M = 0.94$ (b) $\varepsilon = 0.2, v_M = 0.94$

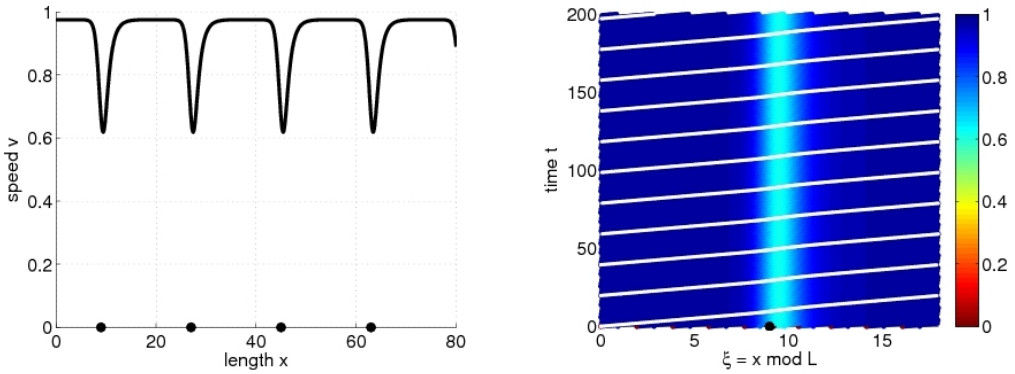

(c) $\varepsilon = 0.3, v_M = 0.91$ (d) $\varepsilon = 0.3, v_M = 0.91$

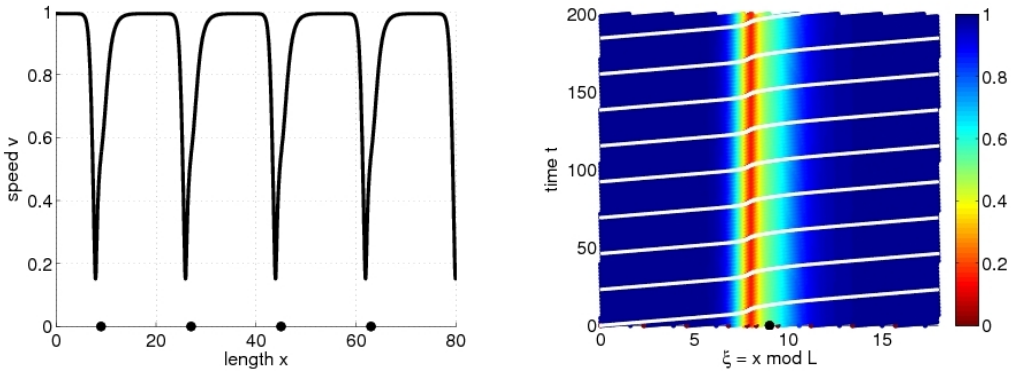

(e) $\varepsilon = 0.3, v_M = 0.78$ (f) $\varepsilon = 0.3, v_M = 0.78$

Figure 8.12: $N = 10$. Stable POMs for $L = 18$ and different ε: Speed versus length (left) and macroscopic view (right) with a trajectory of a single car in white. The position of the bottleneck and its size (right) are indicated by black circles. Note that for $\varepsilon = 0.3$ there are two different stable POMs.

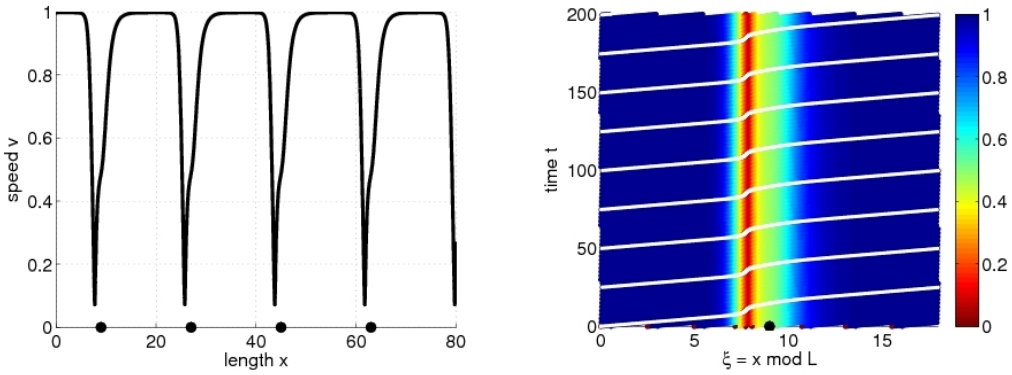

(a) $\varepsilon = 0.4, v_M = 0.72$ (b) $\varepsilon = 0.4, v_M = 0.72$

Figure 8.13: $N = 10$. Stable POMs for $L = 18$ and $\varepsilon = 0.4$: Continuation of figure 8.12

wave. In our new context this solution is a quasi-POM. Its traveling wave dynamics is visualized in figure 8.14(a) and figure 8.14(b). The corresponding invariant curve can be seen in figure 8.17(a). We expect that this special quasi-POM for $\varepsilon = 0$ is perturbed to quasi-POMs for $\varepsilon > 0$.

Indeed, for various values of ε with $0 < \varepsilon < \varepsilon_N$ we found quasi-POMs by simulation. Figures 8.14-8.16 show how the macroscopic speed-pattern is changed due to increasing ε from $\varepsilon = 0$ (traveling wave) to $\varepsilon = 0.35$ (POM). There is an interaction of the traveling wave with the bottleneck. For $\varepsilon \in [0, 0.24]$ the traveling wave structure of the Hopf-periodic wave persists. For larger bottleneck strength ($\varepsilon \geq 0.25$) the traveling wave structure does not exist anymore. There appears more than one congestion upstream the bottleneck and a rather free-flowing traffic downstream.

Similar to POMs for $L = 18$, a coexistence of two different stable dynamics was found for $L = 13$. Looking more thoroughly on the last two rows in figure 8.16 we see that there is a coexistence of two qualitatively different quasi-POMs for $\varepsilon = 0.25$, one of which – the second – seems to be the "Neimark–Sacker-successor" of quasi-POMs emanating in ε_N, the other the "Hopf-successor" of quasi-POMs emanating in $\varepsilon = 0$. One should also compare the corresponding invariant curves in figure 8.17(c) and figure 8.17(d). The quasi-POM visualized in figure 8.17(d) seems to have less dramatic dynamics since the headways are farther away from zero than that in figure 8.17(c). On the other hand, this quasi-POM has a slightly less average speed v_M than the other. Obviously, in figure 8.15(d) on each round a car trajectory (in white) in general passes two congestions upstream the bottleneck while the trajcetory in figure 8.15(b) crosses only one jam area (dark red) in each round which is in general "stronger" than the jam areas in figure 8.14.

Again, let us mention a possible analogy to the theory of Kerner (2008). The quasi-POMs with traveling wave character in figure 8.14 seem to be realizations of the so called jam phase whereas the "fixed" (at the bottleneck) quasi-POMs in figure 8.15(c,d) and 8.16 make part of the congested phase. A possible passage from a "fixed" quasi-POM to a traveling wave quasi-POM (by changing the density) would correspond to the so called pinch effect in the Kerner theory. However let us underline that the results of Kerner are based on much more complex stochastic multi-phase and multi-lane theory.

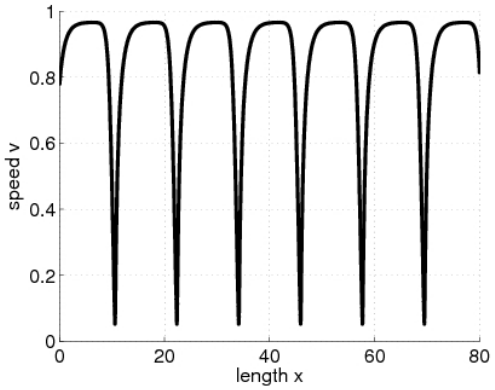

(a) Hopf-periodic dynamics. $\varepsilon = 0, v_M = 0.67$

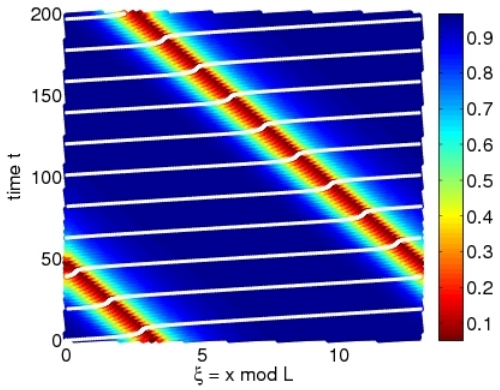

(b) Macro view of (a). $\varepsilon = 0, v_M = 0.67$

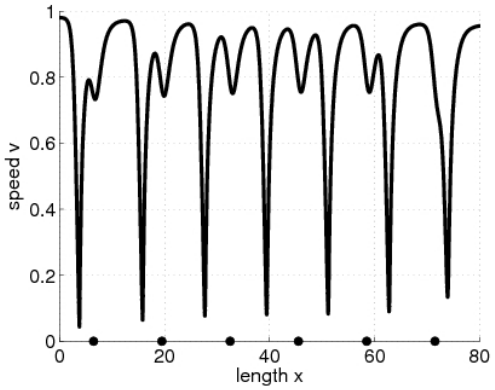

(c) $\varepsilon = 0.2, v_M = 0.65$

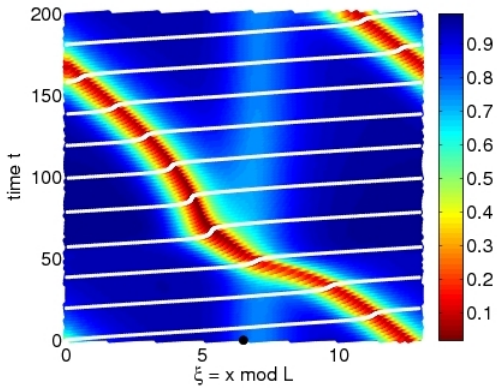

(d) $\varepsilon = 0.2, v_M = 0.65$

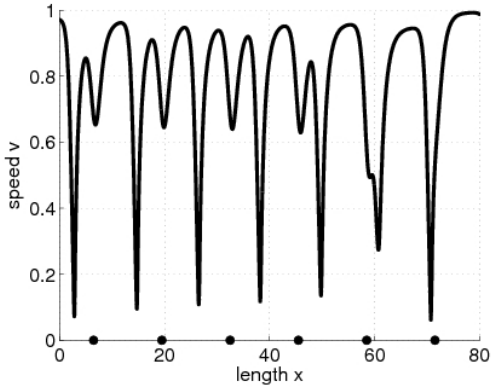

(e) $\varepsilon = 0.24, v_M = 0.65$

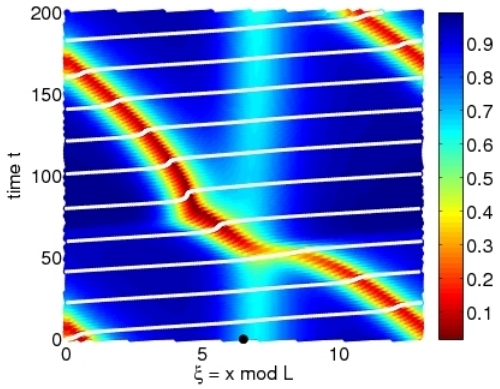

(f) $\varepsilon = 0.24, v_M = 0.65$

Figure 8.14: $N = 10, L = 13$. Quasi-POMs and their average speeds v_M for $0 \leq \varepsilon \leq 0.25$: Speed versus length (left) and macroscopic views (right). The position of the bottleneck is indicated by black circles.

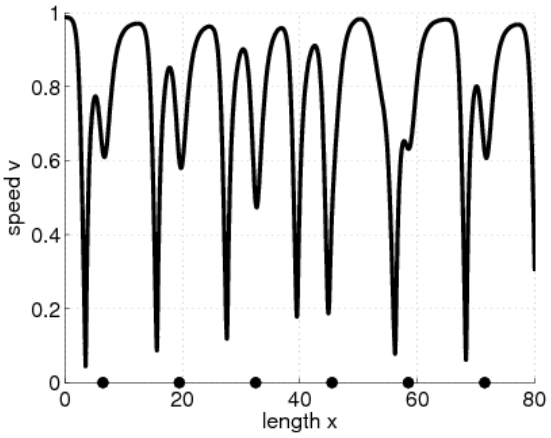

(a) $\varepsilon = 0.25, v_M = 0.64$

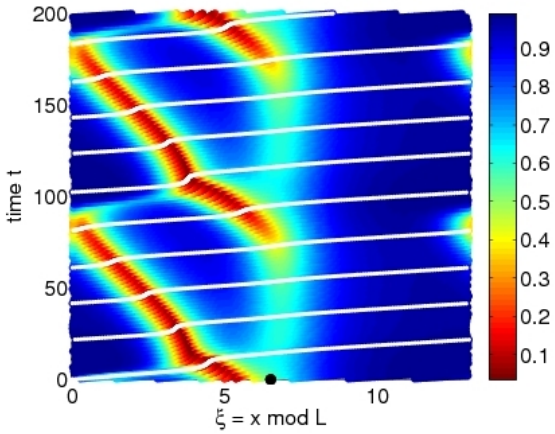

(b) $\varepsilon = 0.25, v_M = 0.64$

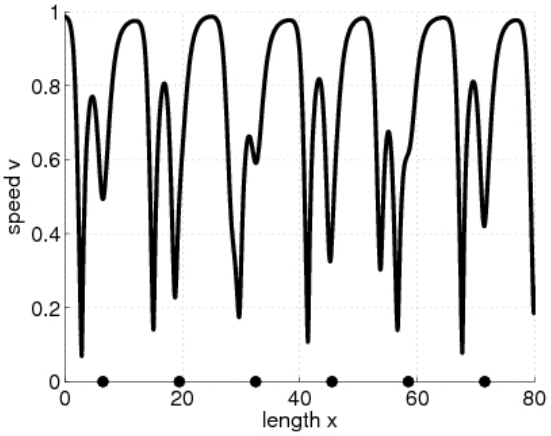

(c) $\varepsilon = 0.25, v_M = 0.61$

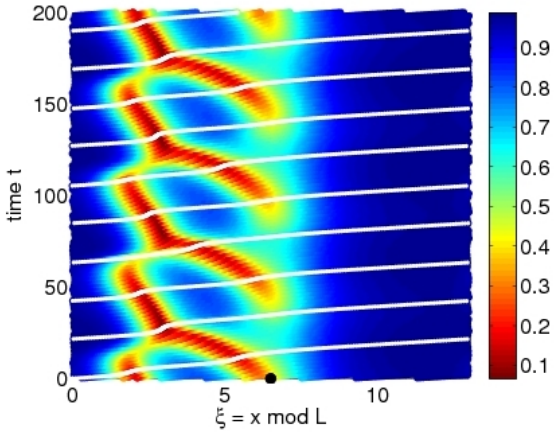

(d) $\varepsilon = 0.25, v_M = 0.61$

Figure 8.15: $N = 10, L = 13$, quasi-POMs. Continuation of figure 8.14. Coexistence of two different quasi-POMs for $\varepsilon = 0.25$.

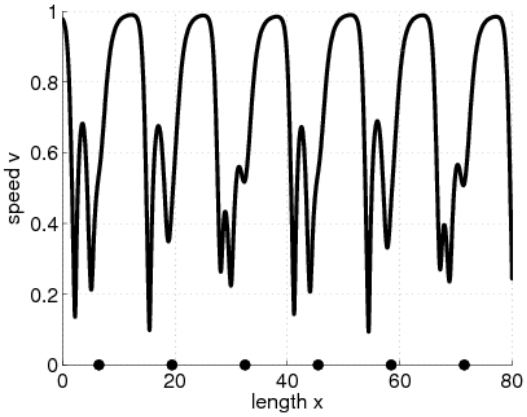

(a) $\varepsilon = 0.3, v_M = 0.59$

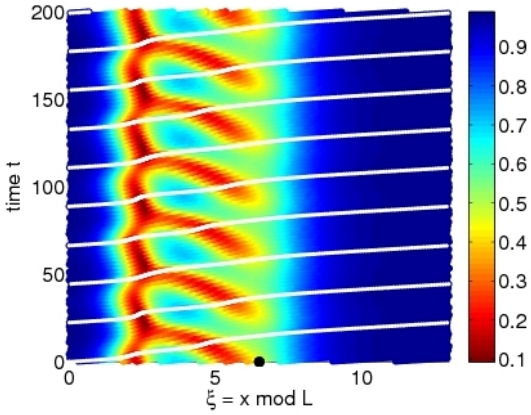

(b) $\varepsilon = 0.3, v_M = 0.59$

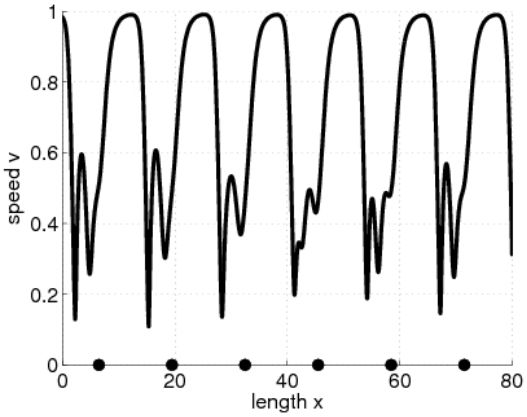

(c) $\varepsilon = 0.33, v_M = 0.57$

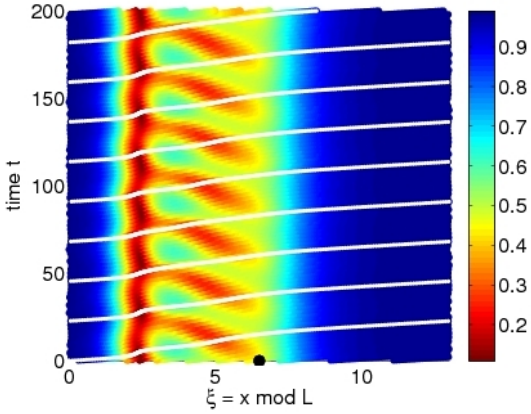

(d) $\varepsilon = 0.33, v_M = 0.56$

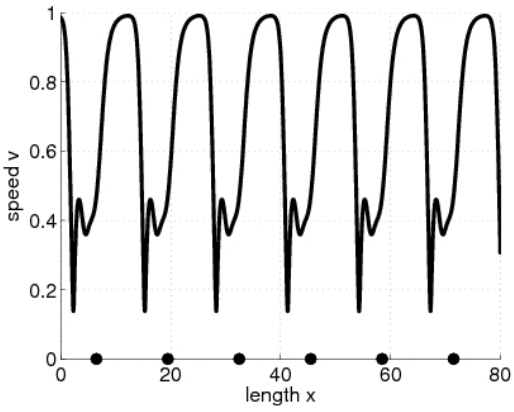

(e) POM for $\varepsilon = 0.35$. $v_M = 0.56$

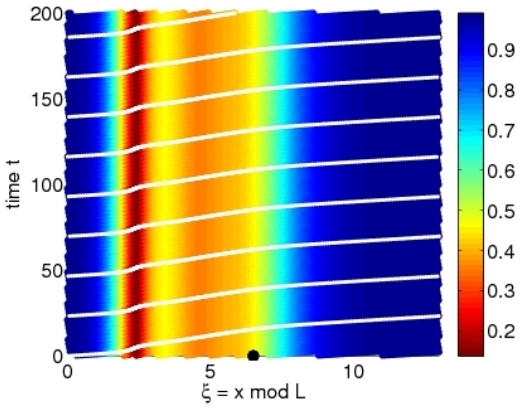

(f) POM for $\varepsilon = 0.35$. $v_M = 0.56$

Figure 8.16: $N = 10, L = 13$, (quasi-)POMs. Continuation of figure 8.15.

Invariant curves

To analyze the type of irregularity of a certain dynamics one has to look at the orbit of the (reduced) Poincaré map. If the limit set of the orbit is a closed invariant curve, we have the dynamics of a quasi-POM. A Neimark–Sacker bifurcation leads to such bifurcating invariant curves. Figure 8.17 shows projections of the invariant curves on the speed-headway plane of the fourth car, counted from the observation place at the measure point ($\xi = 0$). Since there are $N = 10$ cars, we expect that the 4th car is rather close to the center of the bottleneck having hence a more interesting dynamics than cars far away.
There is still no powerful numerical tool to continue invariant curves of quasi-POMs as a function of parameters. If this would be available, we guess that there might be a S-shaped branch of quasi-POMs with respect to ε connecting the quasi-POMs of Neimark–Sacker type and that of Hopf-type and possessing two folds near $\varepsilon = 0.25$.

8.3.3 Other values of L

Up to now we have chosen mainly $L = 13$ and $L = 18$ and $0 \leq \varepsilon \leq 0.5$. Our dynamical simulations yielded POMs and quasi-POMs, nothing else. This is different for smaller values of L where we guess more complex dynamics.
Figure 8.18(a) shows a chaotic like pattern for $L = 8$ — no time-periodicity is observed. Figure 8.18(b) shows a quasi-POM which may be due to a period-doubling process in increasing ε from $\varepsilon = 0$ to $\varepsilon = 0.3$ for $L = 10$.

8.3.4 More pictures

See figures 8.19-8.21.

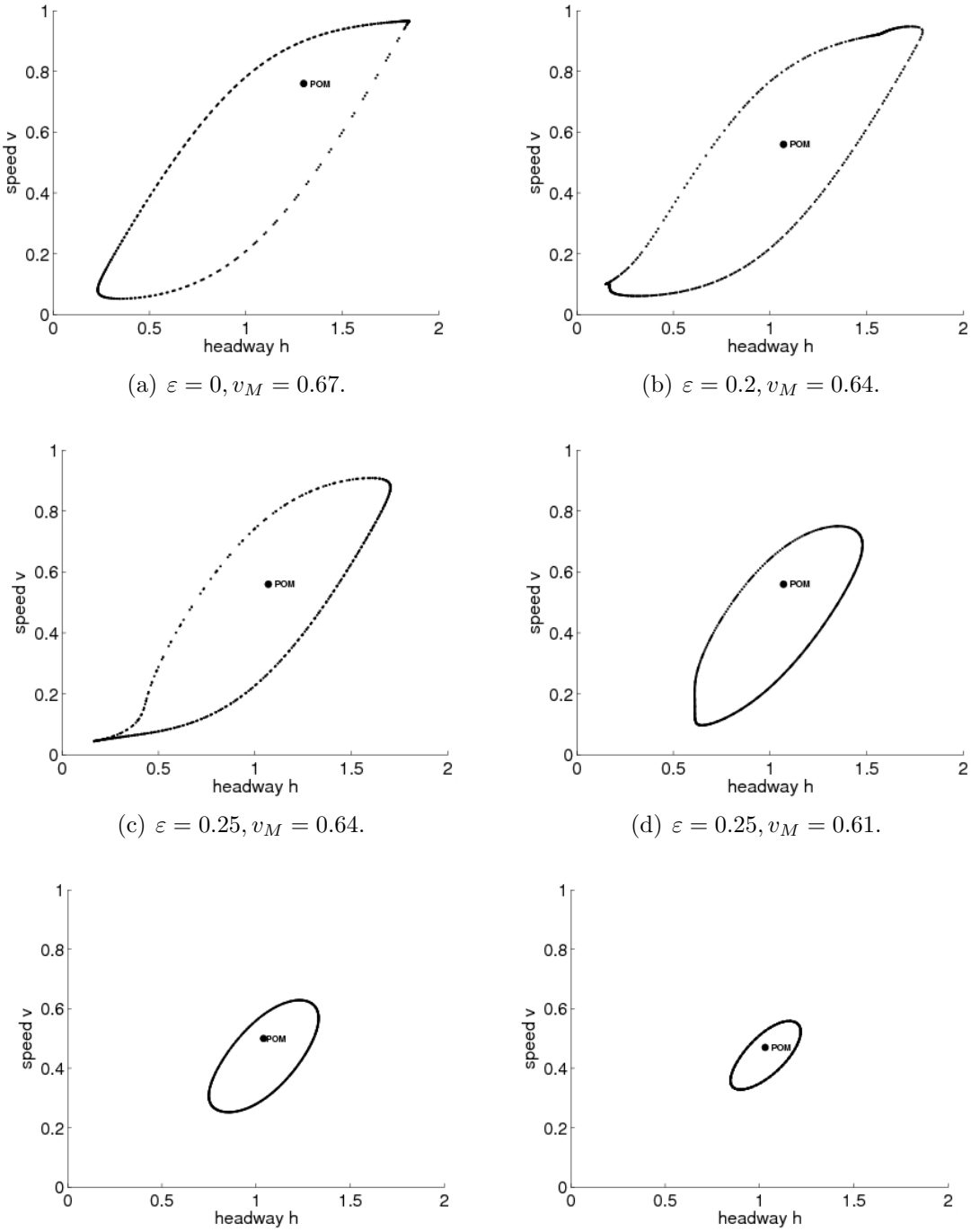

(a) $\varepsilon = 0, v_M = 0.67$.

(b) $\varepsilon = 0.2, v_M = 0.64$.

(c) $\varepsilon = 0.25, v_M = 0.64$.

(d) $\varepsilon = 0.25, v_M = 0.61$.

(e) $\varepsilon = 0.3, v_M = 0.59$.

(f) $\varepsilon = 0.33, v_M = 0.56$

Figure 8.17: $N = 10, L = 13, 0.0 \leq \varepsilon \leq 0.33$. Visualization of quasi-POMs in figures 8.14-8.16 by invariant curves of the reduced Poincaré map for car No. 4, $L = 13$ and different values of ε. The unstable POMs are marked.

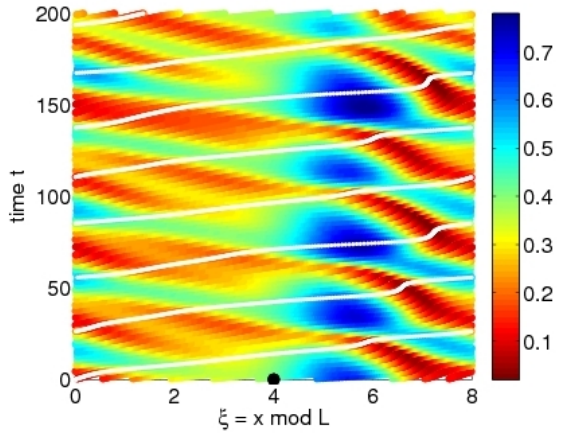

(a) $L = 8, \varepsilon = 0.4, v_M = 0.28$. Chaos?

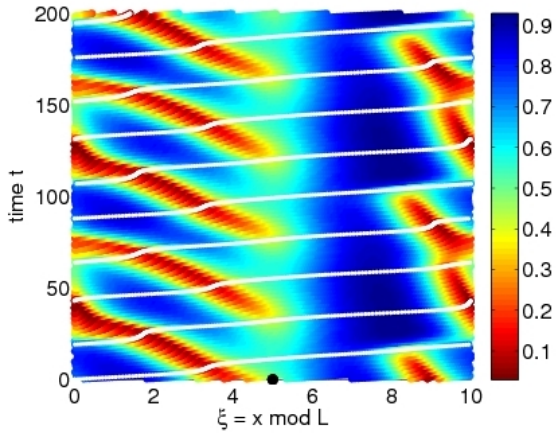

(b) $L = 10, \varepsilon = 0.3, v_M = 0.45$: Quasi-POM. Result of period doubling ?

Figure 8.18: $N = 10$. Macroscopic visualization of two complex dynamics for $L = 8$ and $L = 10$

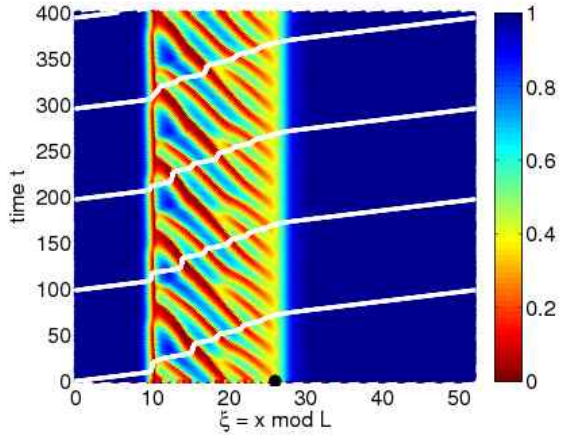

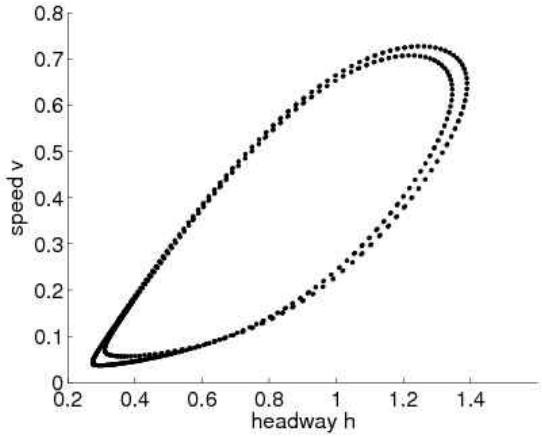

Figure 8.19: $N = 40, L = 52, \varepsilon = 0.4, v_M = 0.41$

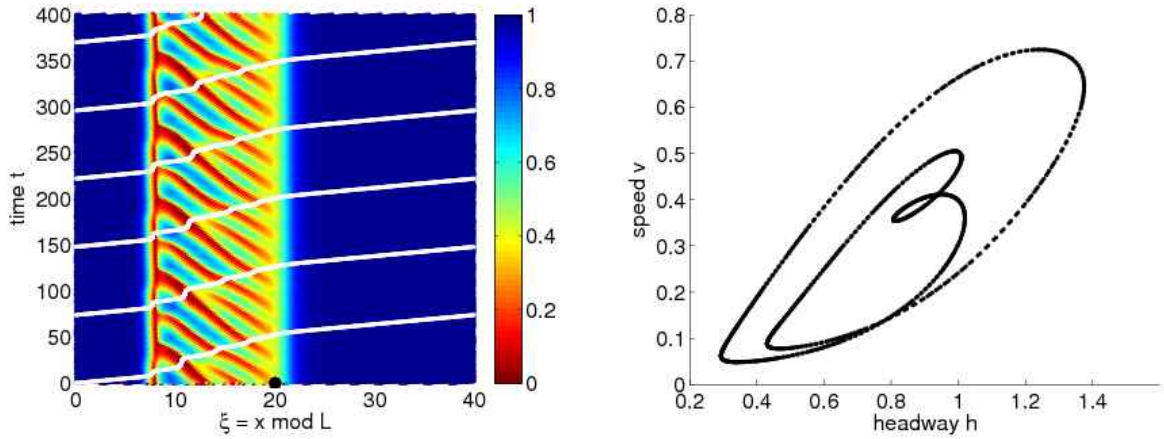

Figure 8.20: $N = 30, L = 40, \varepsilon = 0.4, v_M = 0.40$

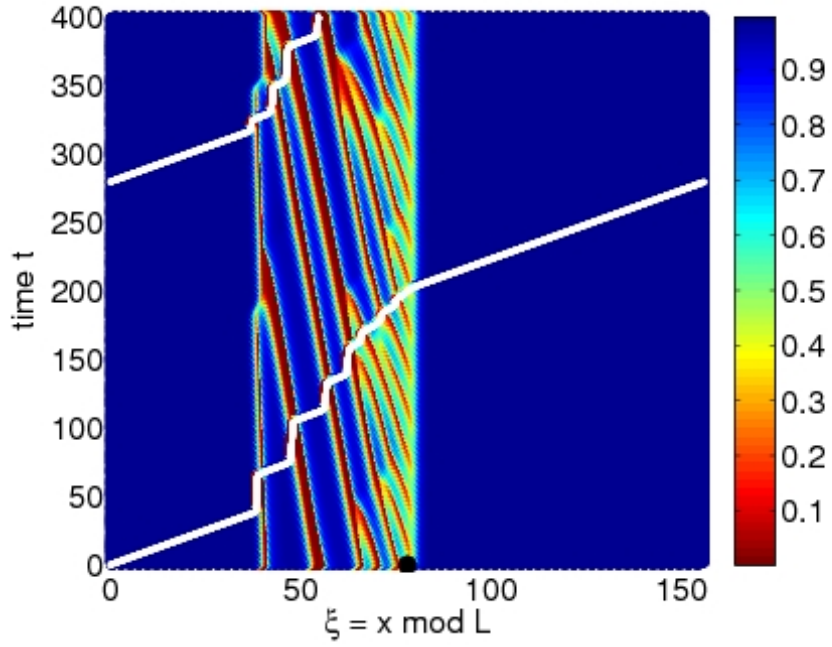

Figure 8.21: Chaos (?): $N = 120, L = 156, \varepsilon = 0.35$

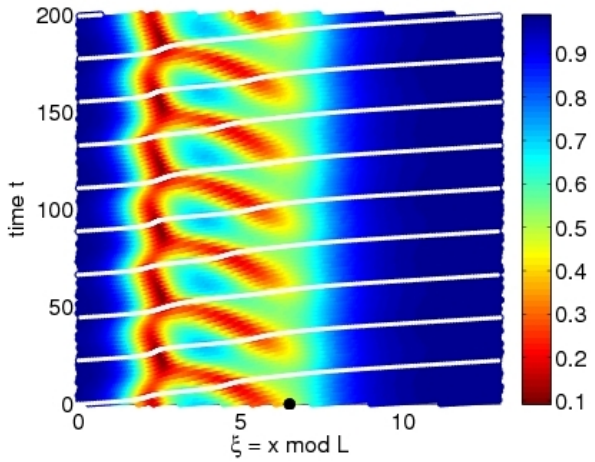

Figure 8.22: $N = 10, L = 13, \varepsilon = 0.3$: Macroscopic visualization of a quasi-POM from [GW10]

8.4 Theory: Quasi-POMs and macroscopic time-periodicity

The following has not yet been published. We sketch the ideas.

Our focus here is on quasi-POMs which bifurcate from Ponies-on-a-Merry-Go-Round-solutions (POMs). The bifurcation parameter are the strength ε of the bottleneck or the length L of the circle.

Quasi-POMs correspond to invariant curves of reduced Poincaré maps, while POMs correspond to their fixed points. Quasi-POMs may be the bifurcation result of Neimark-Sacker type. A reduced Poincaré map π involves an observer somewhere at a measure point $\xi \in S^1_L$ which we assume to be $\xi = 0$, opposite to the bottleneck.

We have experienced a time-periodic pattern in the macroscopic visualization of quasi-POMs. For an example from [GW10] look at Fig. 8.16(b), shown again in figure 8.22. The time-periodicity is obvious.

This observed macroscopic time periodicity can be proved, by analyzing the invariant curves γ associated with the quasi-POMs using dynamical system theory for circle maps, see Ch. 5.1. Yet, we had no traffic interpretation of γ. We only used the invariant curves for the classification of the dynamics as quasi-POMs.

The projection of the corresponding invariant curve on the speed-headway plane of a suitable car close to the center of the bottleneck is shown in Fig. 8.23. Here also the first 10 orbit points under the reduced Poincaré map are numbered. The rather small angle difference of two successive points of the orbit indicates a rather small *rotation number* ($\varrho = 0.068$), see below.

The invariant curve, called γ, is living in $\mathbb{R}^{2N-1}$, where N is the number of cars. Every $x \in \gamma$ is a possible observed configuration of the whole car ensemble. Introducing suitable angle coordinates, the flow of our ODE system, restricted to γ, can be interpreted as an orientation preserving diffeomorphism f of the circle $S^1 := \mathbb{R}/\mathbb{Z}$. The classical theory of such circle maps is well known, see DE MELO, VAN

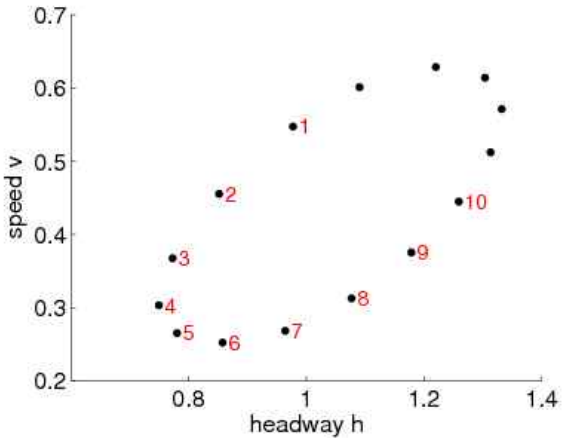

Figure 8.23: $N = 10, L = 13, \varepsilon = 0.3$. Invariant curve for car No.4

Strien [dMvS91], Guckenheimer-Holmes [GH83], but also Ch. 5.1. The most prominent notion is that of a **rotation number** $\varrho \in [0, 1)$ (Ch. 5.3).
We have to assume that ϱ is *sufficiently irrational* or with other words that ϱ is *badly approximable by rational numbers*. This is guaranteed by certain Diophantine equation[1], see Guckenheimer-Holmes p.302 [GH83] or de Melo - van Strien [dMvS91]. From this assumption which we do not explain in detail, one can conclude that f is diffeo-conjugate to a rotation about the angle ϱ. Further, we use the ergodicity of a circle map with irrational rotation number by applying the Birkhoff Ergodic Theorem (see de Melo, van Strien p.50 [dMvS91]), which claims that for all continuous functions g on γ the time average

$$\lim_{n\to\infty} \frac{1}{n} \sum_{j=0}^{n-1} g(f^j(\phi_0)) = \int_\gamma g d\mu \text{ for all } \phi_0 \tag{8.35}$$

exists[2] and equals the space average of g.

An obvious guess is that the time-period T_p of the macroscopic pattern equals the average time an orbit under f needs to circle γ (time of circulation). We can prove

$$T_p = \frac{\tau}{\varrho} \tag{8.36}$$

where τ is the average wait time the observer has to wait between two successive passings of cars. τ exists due to the Birkhoff Ergodic Theorem and has a simple traffic relevance, since the global flow f of the dynamics is given by

$$f = \frac{1}{\tau} = \frac{1}{\varrho \cdot T_p}. \tag{8.37}$$

Further, there is a numerical algorithm, due to MacKay [Mac92] by which the rotation number can be efficiently computed. More precisely: The rotation number ϱ can be included by convergents of

[1] $\exists \varepsilon, c > 0 : \left| \varrho - \frac{p}{q} \right| \geq \frac{c}{q^{2+\varepsilon}} \forall p, q \in \mathbb{N}$.

[2] The convergence is uniformly wrt to the initial point ϕ_0.

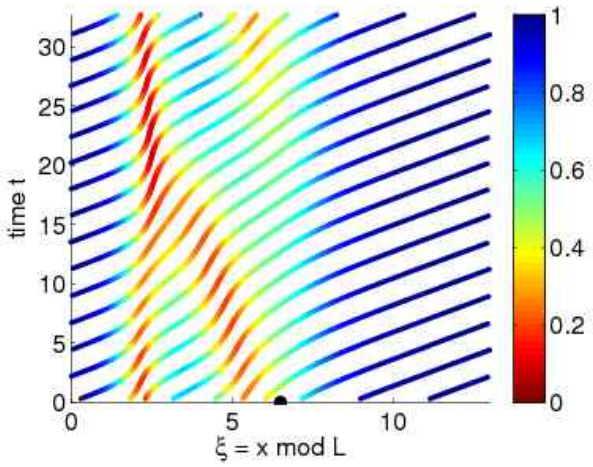

Figure 8.24: Discrete macroscopic visualization of a quasi-POM (MakroN10L13ep0,3SingleOrbits)

the continuous fraction expansion of ϱ. It turns out that this algorithm can be extended to compute the period T_p.

As another consequence, having computed T_p, we can associate with the discrete traffic flow a macroscopic continuous speed function $v(\xi, t)$ being T_p-periodic in the time variable and interpolating the discrete trajectories $v(\xi_j(t), t), j = 1, 2, ..., N$. Fig. 8.22 is not very suitable to see the discrete trajectories of our macroscopic visualization since time runs through a too large time interval. More convincing is Fig. 8.24 where the trajectories are shown only for $t \in [0, T_p]$ with $T_p = 32.7$.

This macroscopic function $v(\xi, t)$ can be numerically approximated by a simple numerical simulation of the ODE system over a certain number m of time intervals of length T_p, time running from $t = 0$ to $t = m \cdot T_p$ and setting

$$v(x_j(t) \bmod L, t \bmod T_p) = \dot{x}_j(t), 1, 2, ..., N, \quad 0 \le t \le m \cdot T_p. \tag{8.38}$$

We call the method to compute $v(\xi, t)$ by (8.38) *projection method*. With respect to a satisfactory visualization we would like to get a set $\{x_j(t) \bmod L, t \bmod T_p)), j = 1, 2, ..., N, t \in [0, m \cdot T_p]\}$ being optically dense in $[0, L] \times [0, T_p]$. The number m being needed for this purpose depends on properties of ϱ and on the chosen thickness of the visualized trajectories. The smaller ϱ and the more irrational ϱ is, the smaller m. For the example in Fig. 8.22-8.24 ($T_p = 32.7$) the continuous result in Fig. 8.25 has been obtained for $m = 10$, i.e. the simulation was performed from $t = 0$ until $t = 10 * T_p = 327$.

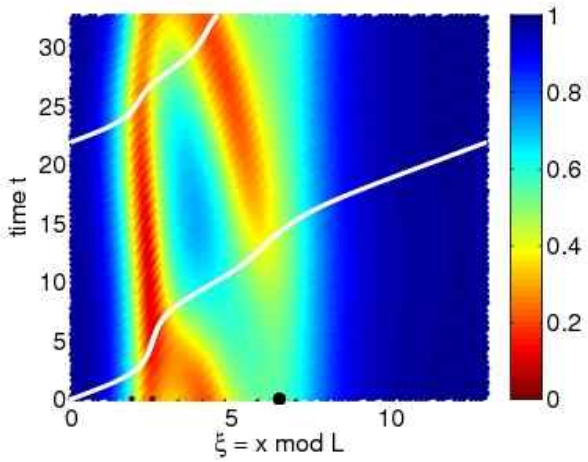

Figure 8.25: $N = 10, L = 13, \varepsilon = 0.3, T_p = 32.7$, quasi-POM: Macroscopic visualization of $v(\xi, t)$ by projection

Bibliography

[AG90] G. Allgower and K. Georg. *Numerical Continuation Methods. An Introduction.* Springer, 1990.

[AGMP91] D. G. Aronson, M. Golubitsky, and J. Mallet-Paret. Ponies on a merry-go-round in large arrays of josephson junctions. *Nonlinearity*, 4:903–910, 1991.

[Arn88] V.I. Arnol'd. *Geometrical Methods In The Theory Of Ordinary Differential Equations.* Springer, 1988.

[BHN+95] M. Bando, K. Hasebe, A. Nakayama, A. Shibata, and Y. Sugiyama. Dynamical model of traffic congestion and numerical simulation. *Phys. Rev. E*, 51:1035ff, 1995.

[Dev92] R.L. Devaney. *A first course in chaotic dynamical systems.* Addison–Wesley, 1992.

[dMvS91] W. de Melo and S. van Strien. *One-dimensional Dynamics.* Springer, 1991.

[DPC+01] E. J. Doedel, R. C. Paffenroth, A. R. Champneys, T. F. Fairgrieve, Yu. A. Kuznetsov, B. Sandstede, and X. Wang. Auto2000: Continuation and bifurcation software for ordinary differential equation (with homcont). Technical report, Caltech, 2001.

[GH83] J. Guckenheimer and P. Holmes. *Nonlinear Oscillations, Dynamical Systems and Bifurcations of Vector Fields.*, volume 42 of *Applied Mathematical Sciences.* Springer, 1983.

[Gov00] W. Govaerts. *Numerical methods for bifurcations of dynamical equilibria.* SIAM, 2000.

[GSW04] I. Gasser, G. Sirito, and B. Werner. Bifurcation analysis of a class of 'car following' traffic models. *Physica D*, 197/3-4:222–241, 2004.

[GW10] I. Gasser and B. Werner. Dynamical phenomena induced by bottleneck. *Philosophical Transactions of the Royal Society A (Special Issue Highway Traffic - Dynamics and Control)*, 2010.

[Kuz98] Y. A. Kuznetsov. *Elements of Applied Bifurcation Theory.*, volume 112 of *Applied Mathematical Sciences.* Springer, 1998.

[Mac92] R.S. MacKay. Rotation interval from a time series. *J. Phys.*, A 20:587–592, 1992.

[MP97] R. Mahnke and N. Pieret. Stochastic master-equation approach to aggregation in freeway traffic. *Phys. Rev. E 56, 2666*, 1997.

[SGW09] T. Seidel, I. Gasser, and B. Werner. Microscopic car-following models revisited: from road works to fundamental diagrams. *SIAM J. Appl. Dyn. Sys. 8, 1305-1323*, 8 (3):1305–1323, 2009.